Buffer–Aided Relaying with Outdated CSI

Toufiqul Islam, *Member, IEEE*, Diomidis S. Michalopoulos, *Senior Member, IEEE*, Robert Schober, *Fellow, IEEE*, and Vijay Bhargava, *Life Fellow, IEEE*

***Abstract*—Adaptive link selection for buffer–aided relaying can provide significant performance gains compared to conventional relaying with fixed transmission schedule. For fixed rate transmission, significant gains in error rate and/or throughput performance have been observed compared to conventional relaying when perfect channel state information (CSI) is available for link selection. However, in practice, link selection may have to be performed based on outdated CSI, because of infrequent feedback of CSI. In this paper, we study the effect of outdated CSI on the error rate performance of adaptive link selection for a three node decode–and–forward (DF) relay network with fixed–rate transmission. In particular, we propose two protocols for link selection. The first protocol does not require knowledge of the reliability of the CSI estimates whereas the second protocol does. For both protocols, we provide a unified error-rate analysis in terms of a decision threshold β, which can be adjusted to maintain buffer stability. In particular, we obtain closed–form expressions for the error rates, and derive asymptotic approximations which reveal the diversity and coding gains. Since packet transmission delay is unavoidable for opportunistic link selection, we analyze the average delay considering both finite and infinite buffer size. We also calculate the throughput for the proposed protocols. The average delay and throughput are functions of the decision threshold β which can be optimized to minimize the error rate while satisfying average delay and/or throughput constraints. Numerical results manifest that even with outdated CSI, adaptive link selection provides a significant coding gain advantage over conventional DF relaying. Furthermore, we show that a diversity gain of two can be achieved for perfect CSI and the optimum error rate can be approached with small delay and/or high throughput.**

***Index Terms*—Cooperative diversity, link selection, buffer–aided relaying, average delay, outdated CSI.**

I. Introduction

Conventional decode–and–forward (DF) relay networks [2], [3] employ half–duplex (HD) relays and a pre–fixed transmission schedule. As the link quality is not taken into account for scheduling the transmissions, the end–to–end performance is limited by the bottleneck link. However, if the transmitting nodes can be selected opportunistically based on the link quality, a better error rate and/or throughput performance is expected compared to conventional relaying. This opportunistic scheduling requires buffers at the relays such that the received message can be stored until a good quality transmit channel is observed [4].

Manuscript received June 26, 2014; revised October 26, 2014 and August 30, 2015; accepted October 18, 2015. The review of this paper was coordinated by Dr. Chia–Han Lee. This work has been presented in part at IEEE WCNC 2014, Istanbul, Turkey [1].

Toufiqul Islam was with The University of British Columbia, Vancouver where this work was conducted. He is now at the Huawei Canada Research Center in Ottawa, Canada (email: toufiq@ece.ubc.ca). Diomidis S. Michalopoulos is with Nokia Networks, Munich, Germany (email: dio@ece.ubc.ca). Robert Schober is with The Friedrich–Alexander–University Erlangen–Nuremberg, Germany (email: schober@lnt.de). Vijay Bhargava is with The University of British Columbia, Vancouver, Canada. (email: vijayb@ece.ubc.ca)

Over the last few years, there has been an increasing interest in buffer–aided relaying protocols [5]- [15], in particular for delay tolerant applications. Two buffer–aided relaying schemes were proposed in [5], where the relay is allowed to receive for a fixed number of time slots before it re–transmits to the destination. These schemes show a throughput improvement compared to receiving and re–transmitting in subsequent time slots. A joint cross–layer scheduling and buffer–equipped relay selection problem was considered in [6], where a considerable throughput improvement was reported compared to relaying without buffers. Throughput optimization for adaptive link selection with buffer–aided relaying was studied in [7] and [8] for adaptive and fixed rate transmission, respectively. The authors in [9] observed that if some packet delay is tolerated, the asymptotic throughput can be improved by exploiting relay buffering and relay mobility. In [10], buffer–aided HD relaying was shown to outperform ideal full duplex relaying in some special cases, when the relay employs multiple antennas. We note that [5]– [9] focused on throughput optimization only and the error rate was not considered. In [11] and [12], relay selection was considered, i.e., the relays with the best $S \rightarrow R$ and the best $R \rightarrow D$ channels were selected for reception and transmission, respectively, but adaptive link selection was not employed. The authors in [13] extended the work in [11] and showed that joint relay and link selection can provide additional diversity gains. In [14], the authors reported that buffering at the relay is useful for achieving multihop diversity for independent and identicaly distributed (i.i.d.) multihop links. The authors in [15] proposed a packet selection based transmission scheme for buffer–aided amplify–and–forward relaying and showed that outage probability can be improved compared to traditional relaying with fixed schedule. A critical requirement for the link selection protocols reported in [7], [13]–[15] is the availability of perfect channel state information (CSI) for link selection. However, in practice, the CSI exploited for link selection may be outdated because CSI may not be fed back frequently as it incurs overhead. It is not clear from the literature whether the protocols developed for perfect CSI would also yield optimum performance when only outdated CSI is available. In particular, if the reliability of the outdated CSI is known, we expect that by exploiting this information for link selection, a better error rate performance can be achieved. The impact of outdated CSI for relay selection has been considered in [16]–[19]. However, the effect of outdated CSI on link selection for buffer–aided relaying has not been considered in the literature, yet.

On the other hand, one important aspect of all opportunistic link selection protocols is the increased end–to–end delay. Despite its importance, most of the previous works [11]–[13] on link selection did not consider delay constrained transmission. In [8], the authors proposed delay constrained link selection protocols for throughput optimization for fixed and mixed rate transmission. In [20], the authors considered fixed rate transmission and analyzed the coded error rate and the delay of a buffer–aided relaying protocol operating over frequency–selective channels. It was shown that full diversity and minimum error rate are observed only when a large delay can be tolerated. However, both [8] and [20] assumed perfect CSI and the effect of the unavoidable delay in the feedback link and/or infrequent feedback of CSI was not taken into account. Furthermore, in [8] and [20], the average system delay was calculated considering the queueing delay only. However, as the buffer at the relay can become empty or full, it is possible that successful transmission cannot always take place and silent time slots may occur. This causes an additional end–to–end delay which has not been investigated for adaptive link selection yet. Moreover, it is not clear from the available literature whether full diversity in terms of the error rate performance can be realized if only a small delay can be tolerated for buffer–aided link selection. However, even though the objective is to analyze the error rate in this work, a constraint on throughput is also important to ensure a minimum end–to–end data rate. Hence, studying adaptive link selection for a delay and throughput constrained buffer–aided relay network with outdated CSI and a corresponding error–rate analysis are of great practical value.

In this paper, we consider a three–node relay network where the relay is equipped with a buffer. We propose two link selection protocols for buffer–aided DF relaying for the cases when the reliability of the outdated CSI is known and not known, respectively. To evaluate the proposed protocols, we analyze the error rate, delay, and throughput as relevant performance metrics. Similar to [20], we introduce a decision threshold β in the link selection criterion which can be tuned to ensure stable buffer operation. For both proposed link selection protocols, we provide a unified end–to–end error rate analysis and derive the corresponding diversity and coding gain expressions for outdated and perfect CSI. Calculation of the error rate is not affected by the silent time slots, which, however, influence the delay and throughput. We derive an expression for the average delay of the system considering both the delay due to queueing at the buffer and the delay due to the silent time slots caused by the proposed protocols. Moreover, we also show that the silent time slots constitute outage events and are responsible for a loss in throughput. Interestingly, the three considered performance metrics are connected through and can be controlled via the decision threshold for link selection, β, and our analyses provide insight into this connection. We also provide guidelines for choosing β for achieving buffer stability and for minimizing the error rate for a target delay and throughput constraint.

Notation: In this paper, $\mathcal{E}\{\cdot\}$ and $|\cdot|$ denote statistical expectation and the magnitude of a scalar or the cardinality of a set, respectively. $Q(x) = \frac{1}{\sqrt{2\pi}}\int_x^\infty e^{-\frac{u^2}{2}}du$ is the Gaussian Q–function and $\mathcal{N}(\mu,\sigma^2)$ denotes the Gaussian distribution with mean μ and variance σ^2. $\mathbb{R}^+$ denotes the set of positive real numbers, "r.h.s." denotes the right hand side, "w.r.t." stands for with respect to, and "$\doteq$" denotes asymptotic equivalence.

II. System Model

The considered system consists of a source terminal S, a DF relay R which is equipped with a buffer, and a destination terminal D. The direct link between S and D is not exploited due to heavy attenuation and/or simplicity of implementation. In our model, S and R transmit at a fixed rate determined by the adopted modulation scheme and S has always data to transmit. We assume uncoded transmission over flat–fading links and each transmission frame consists of two phases: a handshaking phase and a data transmission phase, cf. Fig. 1. Furthermore, we assume that the link selection is performed by a control unit (CU) which collects the CSI of both links and feeds the result of the selection process back to the transmitting nodes. Note that depending on the scenario, the source, the relay, the destination or an external node can serve as the CU. During the handshaking phase, the CSI required for link selection is acquired by the CU and the decision regarding the link selection is fed back to the nodes. Pilot symbols are inserted between chunks of data symbols in the data transmission phase. These pilots are used at the receiver, i.e., the relay or the destination, to accurately estimate the channel for coherent detection. To reduce the signalling overhead, the link selection is performed only at the beginning of each frame. Hence, the CSI used for link selection may become outdated during the data transmission phase, and the link selection decision may not be optimal for the transmitted data symbols. As the data transmission phase can be longer than the handshaking phase, the correlation between the channel states used for link selection and data detection may change over time. However, taking into account different correlation values during data transmission would make the delay analysis in this paper highly complicated. Hence, for convenience and to gain basic insight for system design, we assume a fixed correlation value between the channels used for link selection and the channels during data transmission[1]. Note that, the channel gains in different frames are assumed to be independent[2].

A packet, consisting of data and pilot symbols, cf. Fig. 1, is transmitted from S to R at time t_s and at a later time $t_r > t_s$, the decoded packet is re–transmitted from R to D. Here, each buffer element at the relay contains one packet. To facilitate the understanding of the analysis, in the sequel we refer to the duration of each data transmission phase as 'time slot'. In the following, we present the CSI model, the assumptions regarding the buffer operation, and the link selection schemes.

[1]The assumption of a fixed correlation value is accurate for time division multiple access (TDMA) based relaying systems, where a relay is shared by several users for forwarding their information to the base station. The relay has separate buffers for all users to temporarily store the information. Without loss of generality, we can assume a block of one 'pilot' and one contiguous 'data symbols' in Fig. 1 comprises transmission of one user and one frame is composed of the handshaking phase and data transmission of all users in TDMA mode. The information of each user is transmitted according to the link selection decisions obtained at the beginning of transmission (i.e., during the handshaking phase). In this set up, each user can be assumed to observe a fixed correlation value for the channel estimates used for link selection and data detection. However, correlation values used for different users may not be the same, of course.

[2]Similar assumptions in the context of relay selection for outdated CSI were made in [16].

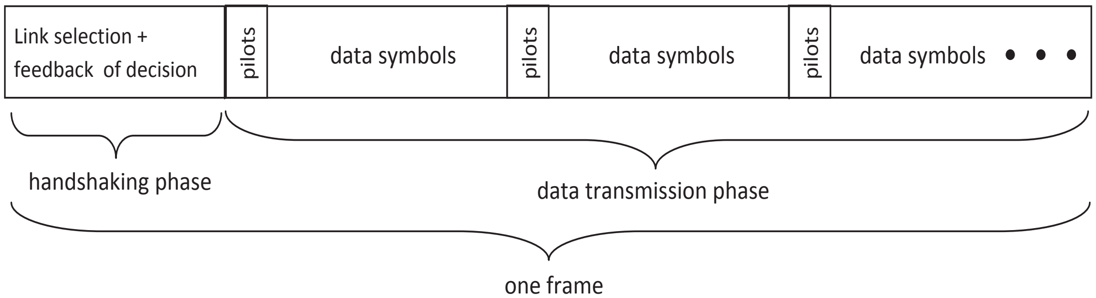

Fig. 1. Each frame consists of two phases: a handshaking phase and a data transmission phase.

A. CSI Model

We denote the flat–fading complex Gaussian channel gain between nodes A and B at time t_z as $h_{AB}(t_z)$, $AB \in \{SR, RD\}$, $z \in \{s, r\}$. $\gamma_{AB}(t_z)$ refers to the instantaneous SNR of link $A \to B$ at time t_z, where $\gamma_{AB}(t_z) \triangleq P_A|h_{AB}(t_z)|^2/N_0$, P_A and N_0 denotes the transmit power of node A and the additive white Gaussian noise variance, respectively. For the rest of the paper, we drop the time index for convenience and it is implicitly assumed that transmission of a packet over the $S \to R$ link takes place earlier than the transmission of the same packet over the $R \to D$ link. γ_{AB} is modelled as an exponentially distributed random variable (RV) with mean $\bar{\gamma}_{AB} = P_A\sigma^2_{AB}\bar{\gamma}$, $AB \in \{SR, RD\}$, where $\bar{\gamma} \triangleq 1/N_0$ and channel gain variance $\sigma^2_{AB} \triangleq \mathcal{E}\{|h_{AB}|^2\}$.

The outdated channel gain used for selection, $\hat{h}_{AB}$, is modelled as [16]

$$\hat{h}_{AB} = \rho_{AB}h_{AB} + \sqrt{1-\rho^2_{AB}}w_{AB}, \tag{1}$$

where w_{AB} is a circularly symmetric complex Gaussian RV having the same variance as h_{AB} and ρ_{AB} is the correlation coefficient between $\hat{h}_{AB}$ and h_{AB}, which, following Jakes' auto–correlation model [21], is given by $\rho_{AB} = J_0(2\pi f_{d,AB}T_d)$. Here, $J_0(\cdot)$ denotes the zeroth order Bessel function of the first kind, $f_{d,AB}$ denotes the Doppler shift on the $A \to B$ link, and T_d is the time difference between the link selection process and data transmission. ρ_{SR} and ρ_{RD} can have different values since the relative speeds of the relay with respect to the source and the destination are not necessarily identical, which causes the Doppler shifts to be different. The estimated SNR is given by $\hat{\gamma}_{AB} = P_A|\hat{h}_{AB}|^2/N_0$. Although $\hat{\gamma}_{AB}$ and γ_{AB} are not necessarily identical, they follow the same distribution with average value $\bar{\gamma}_{AB}$. The joint probability density function (PDF) of γ_{AB} and $\hat{\gamma}_{AB}$ is given by [16]

$$f_{\gamma_{AB},\hat{\gamma}_{AB}}(x,y) = \frac{e^{-\frac{x+y}{\bar{\gamma}_{AB}\left(1-\rho^2_{AB}\right)}}}{\bar{\gamma}^2_{AB}\left(1-\rho^2_{AB}\right)} I_0\left(\frac{2\sqrt{xy}\rho_{AB}}{\bar{\gamma}_{AB}\left(1-\rho^2_{AB}\right)}\right), \tag{2}$$

where $I_0(\cdot)$ denotes the zeroth order modified Bessel function of the first kind.

B. Operation of the Buffer

As the buffering capability at the relay is critical, a stable buffer operation has to be maintained throughout the link selection procedure. For simplicity, we assume that the transmission rates of source and relay, denoted by S_0 and R_0, respectively, are equal. However, this can be generalized and different transmission rates can be incorporated into the analysis. The received packets at the relay are appended to the queue regardless of decoding errors[3]. We assume the queue operates in a First–In–First–Out (FIFO) mode[4].

From queueing theory, we know that for stable operation of the buffer, the length of the queue must not grow over time, i.e., we require the departure rate D to be equal to or higher than the arrival rate A, i.e., $D \geq A$. For maximization of the throughput, it was shown in [7] that the queue needs to operate at the edge of stability, i.e., when $A = D$. However, for error rate minimization, this condition may not be optimal, as will be shown in Section IV. Furthermore, we can control the arrival rate to limit the average delay. It was shown in [20] that for fixed rate transmission, the average delay is infinite when $A = D$ holds. Hence, we need to operate the queue in the region $D > A$ to achieve a tolerable delay. Now, taking the above considerations into account, we propose two link selection protocols. Analytical expressions for A and D for finite and infinite buffer sizes are presented in Section IV, where we study the end–to–end delay for the system.

C. Link Selection Protocols

For the development of the proposed link selection protocols, we assume the relay is equipped with a buffer of finite size. Depending on whether the reliability of the CSI estimates ρ_{AB}, $AB \in \{SR, RD\}$, is known or not, we formulate two link selection protocols. Protocol 1 depends on the instantaneous outdated SNR only, whereas Protocol 2 considers both the instantaneous outdated SNR and the reliability of the estimates.

1) Protocol 1: For M–ary phase shift keying (PSK), M–ary quadrature amplitude modulation, M–ary frequency shift keying, and high values of SNR, the symbol error rate (SER) of the $A \to B$ link can be expressed as [24]

$$P_B(e) = \mathcal{E}_{\gamma_{AB}}\{CQ(\sqrt{\eta\gamma_{AB}})\}, \tag{3}$$

[3]Allowing the relay to forward erroneous packets is delay efficient and is not uncommon in the literature. For conventional DF relay networks, it was shown in [22], [23] that with intelligent combining at the destination and/or link adaptation, full diversity can still be achieved even if the relays forward erroneous packets. Note that it is also possible that the relay appends packets to the queue only if the decoding is successful. However, this assumption will completely change the link selection procedure and delay analysis and is not considered here.

[4]We note that the FIFO mode is appropriate if the packets do not have individual delay requirements. If the packets do have individual delay requirements, packets with more stringent delay requirements can be moved to the head of the queue to decrease their end–to–end delay. This does not affect the error rate, delay, and throughput averaged over all packets, i.e., the analyses presented in Sections III–V are still valid.

TABLE I
LINK SELECTION PROTOCOLS.

Case	Buffer status	Link quality (Protocol 1)	Link quality (Protocol 2)	Selected link
1	Empty	$\hat{\gamma}_{SR} < \beta\hat{\gamma}_{RD}$	$\hat{\gamma}_{SR} < l_1$ for Case a $\hat{\gamma}_{RD} \geq l_2$ for Case b	None
2	Not empty	$\hat{\gamma}_{SR} < \beta\hat{\gamma}_{RD}$	$\hat{\gamma}_{SR} < l_1$ for Case a $\hat{\gamma}_{RD} \geq l_2$ for Case b	$R \to D$
3	full	$\hat{\gamma}_{SR} \geq \beta\hat{\gamma}_{RD}$	$\hat{\gamma}_{SR} \geq l_1$ for Case a $\hat{\gamma}_{RD} < l_2$ for Case b	None
4	Not full	$\hat{\gamma}_{SR} \geq \beta\hat{\gamma}_{RD}$	$\hat{\gamma}_{SR} \geq l_1$ for Case a $\hat{\gamma}_{RD} < l_2$ for Case b	$S \to R$

where C and η are modulation dependent parameters. As $Q(\sqrt{\eta\gamma_{AB}})$ monotonically decreases with increasing γ_{AB}, activating the link with the highest γ_{AB} minimizes the instantaneous error rate. However, due to buffer stability issues, we cannot perform link selection based on instantaneous CSI only. Instead, we select the $S \to R$ link when

$$\gamma_{SR} \geq \beta\gamma_{RD}, \tag{4}$$

otherwise, the $R \to D$ link is selected. Parameter $\beta \in \mathbb{R}^+$ in (4) can be adjusted to balance the selection of both links to ensure buffer stability. Furthermore, by tuning β, we can also guarantee certain average delay and throughput constraints as will be discussed in Section VI. However, in practice, perfect CSI may not be available, and we have to rely on outdated CSI for link selection. Hence, for outdated CSI, the $S \to R$ link is selected when

$$\hat{\gamma}_{SR} > \beta\hat{\gamma}_{RD}, \tag{5}$$

otherwise, the $R \to D$ link is selected. Furthermore, the buffer may be either empty or full at times. If an empty (full) buffer is encountered and the $R \to D$ ($S \to R$) link is selected, no transmission takes place and a silent time slot results. Here, unlike the protocol in [20], we do not force the source or the relay to transmit during the silent time slots because in this case, transmission would take place over the weaker link and consequently, the error rate performance would degrade. We summarize the proposed protocol in Table I.

2) Protocol 2: Now, we develop a link selection policy that takes into account the reliabilities of the CSI in both links, i.e., ρ_{SR} and ρ_{RD}. In particular, we develop a link selection policy based on the error rates in both links conditioned on the outdated CSI. The following Proposition provides an expression for the conditional error rate.

Proposition 1: The error rate of the $A \to B$ link conditioned on $\hat{\gamma}_{AB}$ can be approximated as

$$P_B(e|\hat{\gamma}_{AB}) \approx \frac{1}{\mu_{AB}} e^{-\frac{\hat{\gamma}_{AB}\rho_{AB}^2}{\bar{\gamma}_{AB}(1-\rho_{AB}^2)}}, \tag{6}$$

$$\text{where} \quad \mu_{AB} = \frac{2}{1-\sqrt{\frac{\bar{\gamma}_{AB}\eta(1-\rho_{AB}^2)}{2+\bar{\gamma}_{AB}\eta(1-\rho_{AB}^2)}}}.$$

Proof: Please refer to the Appendix A. ■

Now, we are ready to introduce the link selection criterion. Again using parameter β, we select the $S \to R$ link if $P_R(e|\hat{\gamma}_{SR})$ is smaller than $P_D(e|\beta\hat{\gamma}_{RD})$, i.e.,

$$\frac{1}{\mu_{SR}} e^{-\frac{\hat{\gamma}_{SR}\rho_{SR}^2}{\bar{\gamma}_{SR}(1-\rho_{SR}^2)}} \leq \frac{1}{\mu_{RD}} e^{-\frac{\beta\hat{\gamma}_{RD}\rho_{RD}^2}{\bar{\gamma}_{RD}(1-\rho_{RD}^2)}}, \tag{7}$$

otherwise the $R \to D$ link is selected. Note that in (7), we use β in such a way that the decision depends on a scaled version of $\hat{\gamma}_{RD}$, similar to Protocol 1. The appropriate choice of β will be discussed in Section VI. Here, $\beta = 1$ means that the link is selected based on the 'actual' conditional error rates. However, as argued for Protocol 1, we choose the value of β such that buffer stability is maintained, and delay and/or throughput constraints are satisfied. Even though (4) and (7) can be identical for some special cases, as will be shown below, in most cases different values of β may be required for the two protocols to observe a target end–to–end delay or throughput.

After some manipulations from (7), we obtain the criterion for selecting the $S \to R$ link as

$$\frac{\hat{\gamma}_{SR}\rho_{SR}^2}{\bar{\gamma}_{SR}(1-\rho_{SR}^2)} + \log(\mu_{SR}) \geq \frac{\beta\hat{\gamma}_{RD}\rho_{RD}^2}{\bar{\gamma}_{RD}(1-\rho_{RD}^2)} + \log(\mu_{RD}). \tag{8}$$

We study (8) for the following two special cases: **Case** a) $\mu_{SR} \leq \mu_{RD}$ and **Case** b) $\mu_{SR} > \mu_{RD}$. At high SNR, we can further simplify the cases to: **Case** a) $\bar{\gamma}_{SR}(1-\rho_{SR}^2) \leq \bar{\gamma}_{RD}(1-\rho_{RD}^2)$ and **Case** b) $\bar{\gamma}_{SR}(1-\rho_{SR}^2) > \bar{\gamma}_{RD}(1-\rho_{RD}^2)$. After some basic modifications, we summarize the condition for selecting the $S \to R$ link as:

Case a)

$$\hat{\gamma}_{SR} \geq \frac{\bar{\gamma}_{SR}(1-\rho_{SR}^2)}{\rho_{SR}^2}\left(\frac{\beta\hat{\gamma}_{RD}\rho_{RD}^2}{\bar{\gamma}_{RD}(1-\rho_{RD}^2)} + \log\left(\frac{\mu_{RD}}{\mu_{SR}}\right)\right) \triangleq l_1, \tag{9}$$

Case b)

$$\hat{\gamma}_{RD} < \frac{\bar{\gamma}_{RD}(1-\rho_{RD}^2)}{\beta\rho_{RD}^2}\left(\frac{\hat{\gamma}_{SR}\rho_{SR}^2}{\bar{\gamma}_{SR}(1-\rho_{SR}^2)} + \log\left(\frac{\mu_{SR}}{\mu_{RD}}\right)\right) \triangleq l_2, \tag{10}$$

otherwise the $R \to D$ link is selected, cf. Table I where Protocol 2 is summarized.

Remark 1: If the links have the same average SNR and the same reliabilities of the CSI estimates (symmetric links), i.e., $\bar{\gamma}_{SR} = \bar{\gamma}_{RD}$ and $\rho_{SR} = \rho_{RD}$, we observe from (8) that the selection rule simplifies to

$$\hat{\gamma}_{SR} > \beta\hat{\gamma}_{RD}, \tag{11}$$

which is identical to Protocol 1 where only instantaneous outdated CSI was considered for selection. Note that (11) also holds when $\{\rho_{SR}, \rho_{RD}\} \to 0$ and the links have the same average SNR.

Remark 2: When the reliability of the CSI estimates is high, i.e., $\{\rho_{SR}, \rho_{RD}\} \to 1$, the selection rule in (8) simplifies to (11) as well. In this case, the selection rule depends on instantaneous CSI only.

Remark 3: Note that β can be negative for Protocol 2 unlike for protocol 1. When the reliabilities of the CSI estimates are poor, $\{\rho_{SR}, \rho_{RD}\} \to 0$, and $\bar{\gamma}_{SR} < \bar{\gamma}_{RD}$ (cf. Case a, (9)) holds, a negative β is required to balance the selection of the links. On the other hand, $\beta \in \mathbb{R}^+$ always holds for Case b in Protocol 2.

Remark 4: For both protocols, we can observe from (5) and (7)/(8) that an increase in β also increases the probability of selecting the $R \to D$ link over the $S \to R$ link.

Remark 5: Note that when $\beta = 1$, the rule in (7) of Protocol 2 only ensures that the link with the minimum error rate is selected at any time slot. $\beta = 1$ does not guarantee that the end–to–end error rate will be minimized, unless the links are symmetric. The dependence of the error rate on β will be discussed in detail in Sections VI and VII. For independent and non–identically distributed (i.n.d.) fading with dissimilar correlation coefficients, the value of β required for Protocol 2 to achieve a target delay or throughput may be different from that for Protocol 1. In this work, we compare the performance of the two protocols for a fixed delay or throughput, see Section VII. We note that Protocol 2 may not always yield a lower error rate compared to Protocol 1 over the feasible range of β.

Remark 6: From Table I, we observe that the proposed protocols do not allow for transmission during silent time slots, which occur if the buffer is full (empty) and the $S \to R$ ($R \to D$) link is selected for transmission, such that transmission over a poor link can be avoided. On the other hand, silent time slots degrade the throughput and the delay, as the system is losing possible transmission opportunities. Hence, under certain conditions, it may be beneficial to modify the proposed protocols such that S (R) transmits if the buffer is empty (full) when the $S \to R$ ($R \to D$) link SNR is larger than some pre–defined threshold. In Section VII, we discuss this modification of the proposed protocols and simulate its performance.

III. Error Rate Analysis

In this section, we evaluate the end–to–end symbol error rate (SER) of both proposed protocols. In our model, a symbol is received in error at D if a) the $S \to R$ link causes an error and the $R \to D$ link is error free, b) R receives the symbol correctly but the $R \to D$ link causes an error, and c) both links cause errors but the errors do not cancel each other. Thus, the end–to–end error rate can be formulated as

$$\begin{aligned}\tilde{P}(e) &\le P_R(e)(1 - P_D(e)) + P_D(e)(1 - P_R(e)) + P_R(e)P_D(e) \\ &\approx P_R(e) + P_D(e) \triangleq P(e), \end{aligned} \tag{12}$$

where $P_R(e)$ and $P_D(e)$ denote the SER of the $S \to R$ and $R \to D$ links, respectively. Here, $P(e)$ is an upper bound because the case where the errors in both links cancel is not taken into account, and (12) is a tight approximation[5] for high SNR. Note that silent time slots do not contribute to the error rate, which is similar to the DF relaying scheme in [25]. In the following, we derive exact and asymptotic expressions for $P(e)$ in (12) for both considered protocols.

A. Protocol 1

The end–to–end error rate for Protocol 1 is provided in the following proposition.

Proposition 2: For Protocol 1, the end–to–end error rate $P(e)$ is given by (13) at the top of next page. For $\bar{\gamma}_{SR} = a\bar{\gamma}$, $\bar{\gamma}_{RD} = b\bar{\gamma}$, $\bar{\gamma} \to \infty$, where $a \triangleq P_S\sigma_{SR}^2$ and $b \triangleq P_R\sigma_{RD}^2$, we obtain the following asymptotic expression for $P(e)$

$$P(e) \doteq \begin{cases} \frac{3C}{4\eta^2}\frac{(a+b\beta)(b+a\beta)}{a^2b^2\beta\bar{\gamma}^2}, & \text{if } \rho_{SR} = \rho_{RD} = 1 \\ \frac{\mathcal{A}_{SR}}{\bar{\gamma}} + \frac{\mathcal{A}_{RD}}{\bar{\gamma}}, & \text{if } \rho_{SR} < 1 \text{ or } \rho_{RD} < 1 \end{cases} \tag{14}$$

where $\mathcal{A}_{SR}$

$$\triangleq \frac{C(a+b\beta)(1-\rho_{SR}^2)}{2a\eta(b\beta + a(1-\rho_{SR}^2))},\ \mathcal{A}_{RD} \triangleq \frac{C(a+b\beta)(1-\rho_{RD}^2)}{2b\eta(a + b\beta(1-\rho_{RD}^2))}. \tag{15}$$

Proof: Please refer to the Appendix B. ■

From the asymptotic expression for $P(e)$ in (14), we can obtain the diversity and coding gains, which are provided in the following corollary.

Corollary 1: The diversity gain G_d is given by

$$G_d = \begin{cases} 2, & \text{if } \rho_{SR} = \rho_{RD} = 1 \\ 1, & \text{if } \rho_{SR} < 1 \text{ or } \rho_{RD} < 1 \end{cases} \tag{16}$$

and the coding gain G_c is given by

$$G_c = \begin{cases} \left(\frac{3C}{4\eta^2}\frac{(a+b\beta)(b+a\beta)}{a^2b^2\beta}\right)^{-1/2}, & \text{if } \rho_{SR} = \rho_{RD} = 1 \\ (\mathcal{A}_{SR} + \mathcal{A}_{RD})^{-1}, & \text{if } \rho_{SR} < 1 \text{ or } \rho_{RD} < 1 \end{cases} \tag{17}$$

Proof: The expressions for G_d and G_c can be easily obtained by expressing $P(e)$ in (14) in the form of $(G_c\bar{\gamma})^{-G_d}$. ■

Hence, we observe that for perfect CSI, $P(e)$ decays at the rate of $\bar{\gamma}^{-2}$, i.e., buffer–aided relaying with link selection achieves a diversity gain of two[6] (which is the maximum possible diversity gain as there are only two flat–fading links to choose from), whereas for outdated CSI, only a diversity gain of one is observed. This is because in the latter case the probability of selecting the worst link becomes non–negligible which leads to a diversity gain loss. Note that conventional half–duplex DF relaying without link selection also achieves a diversity gain of one [2]. However, it will be shown in Section VII that buffer–aided relaying with adaptive link selection achieves a higher coding gain compared to conventional DF relaying, even if the CSI is outdated.

B. Protocol 2

If the reliability of the CSI estimates is known, we can exploit this information in Protocol 2. As outlined in Section II-C2, we

[5]The term $P_R(e)P_D(e)$ decays faster with increasing SNR than $P_R(e)$ and $P_D(e)$, respectively.

[6]In terms of outage probability, a diversity gain of two was also observed in [8] for fixed rate transmission.

$$
\begin{aligned}
P(e) = {} & C\frac{\bar{\gamma}_{SR}\left(1-\sqrt{\frac{\bar{\gamma}_{SR}\eta}{2+\bar{\gamma}_{SR}\eta}}\right) - \beta\bar{\gamma}_{RD}\sqrt{\frac{\bar{\gamma}_{SR}\eta}{2+\bar{\gamma}_{SR}\eta}} + \beta\bar{\gamma}_{RD}\left(1+\frac{2}{\bar{\gamma}_{SR}\eta}+\frac{2\rho_{SR}^2}{\bar{\gamma}_{SR}\eta(1-\rho_{SR}^2)+\beta\bar{\gamma}_{RD}\eta}\right)^{-\frac{1}{2}}}{2\bar{\gamma}_{SR}} \\
& + C\frac{\beta\bar{\gamma}_{RD}\left(1-\sqrt{\frac{\bar{\gamma}_{RD}\eta}{2+\bar{\gamma}_{RD}\eta}}\right) - \bar{\gamma}_{SR}\sqrt{\frac{\bar{\gamma}_{RD}\eta}{2+\bar{\gamma}_{RD}\eta}} + \bar{\gamma}_{SR}\left(1+\frac{2}{\bar{\gamma}_{RD}\eta}+\frac{2\beta\rho_{RD}^2}{\bar{\gamma}_{SR}\eta+\beta\bar{\gamma}_{RD}\eta(1-\rho_{RD}^2)}\right)^{-\frac{1}{2}}}{2\beta\bar{\gamma}_{RD}}
\end{aligned}
\tag{13}
$$

$$
P(e) = \begin{cases}
\frac{C(1-\rho_{SR}^2)(\beta\rho_{RD}^2(1-\rho_{SR}^2)+\rho_{SR}^2(1-\rho_{RD}^2))}{\mu_{SR}(\beta\rho_{RD}^2+\rho_{SR}^2(1-\rho_{RD}^2)))} + C\frac{\frac{1-\rho_{RD}^2}{\mu_{RD}} - \frac{\left(\frac{\mu_{RD}}{\mu_{SR}}\right)^{-1/\rho_{SR}^2}\rho_{SR}^2(1-\rho_{RD}^2)}{\mu_{SR}(\rho_{SR}^2+\beta(1-\rho_{SR}^2)\rho_{RD}^2)}}{1-\frac{\left(\frac{\mu_{RD}}{\mu_{SR}}\right)^{1-1/\rho_{SR}^2}\rho_{SR}^2(1-\rho_{RD}^2)}{\beta\rho_{RD}^2+\rho_{SR}^2(1-(1+\beta)\rho_{RD}^2)}}, & \text{Case } a \\
C\frac{\frac{1-\rho_{SR}^2}{\mu_{SR}} - \frac{\beta\left(\frac{\mu_{SR}}{\mu_{RD}}\right)^{(-1+\rho_{RD}^2)/\beta\rho_{RD}^2}\rho_{RD}^2(1-\rho_{SR}^2)}{\mu_{SR}(\rho_{SR}^2+(\beta-\rho_{SR}^2)\rho_{RD}^2)}}{1-\frac{\beta\left(\frac{\mu_{SR}}{\mu_{RD}}\right)^{(-1+\rho_{RD}^2)/\beta\rho_{RD}^2}\rho_{RD}^2(1-\rho_{SR}^2)}{\beta\rho_{RD}^2+\rho_{SR}^2(1-(1+\beta)\rho_{RD}^2)}} + \frac{C\left(\frac{\mu_{SR}}{\mu_{RD}}\right)^{-1/\beta}(1-\rho_{RD}^2)(\beta\rho_{RD}^2+\rho_{SR}^2(1-(1+\beta)\rho_{RD}^2))}{\mu_{RD}(\beta\rho_{RD}^2+\rho_{SR}^2(1-\beta\rho_{RD}^2))}, & \text{Case } b
\end{cases}
\tag{18}
$$

study two possible cases: **Case** a) $\bar{\gamma}_{SR}(1-\rho_{SR}^2) \leq \bar{\gamma}_{RD}(1-\rho_{RD}^2)$ and **Case** b) $\bar{\gamma}_{SR}(1-\rho_{SR}^2) > \bar{\gamma}_{RD}(1-\rho_{RD}^2)$, and derive the error rate expressions for each case separately[7]

Proposition 3: For Protocol 2, the end–to–end error rate $P(e)$ is given by (18). For $\bar{\gamma}_{SR} = a\bar{\gamma}$, $\bar{\gamma}_{RD} = b\bar{\gamma}$, $\bar{\gamma} \to \infty$, we obtain an asymptotic expression for $P(e)$ in (18) as

$$
P(e) \doteq \begin{cases}
\frac{3C}{4\eta^2}\frac{(a+b\beta)(b+a\beta)}{a^2b^2\beta\bar{\gamma}^2}, & \text{if } \rho_{SR} = \rho_{RD} = 1 \\
\frac{\mathcal{A}_{1,SR}}{\bar{\gamma}} + \frac{\mathcal{A}_{1,RD}}{\bar{\gamma}}, & \text{if } \rho_{SR} < 1\ ,\ \rho_{RD} < 1,\ \text{Case } a \\
\frac{\mathcal{A}_{1,RD}}{\bar{\gamma}}, & \text{if } \rho_{SR} \to 1\ ,\ \rho_{RD} < 1,\ \text{Case } a \\
\frac{\mathcal{A}_{2,SR}}{\bar{\gamma}} + \frac{\mathcal{A}_{2,RD}}{\bar{\gamma}}, & \text{if } \rho_{SR} < 1\ ,\ \rho_{RD} < 1,\ \text{Case } b \\
\frac{\mathcal{A}_{2,SR}}{\bar{\gamma}}, & \text{if } \rho_{SR} < 1\ ,\ \rho_{RD} \to 1,\ \text{Case } b
\end{cases}
\tag{19}
$$

where $\mathcal{A}_{1,SR}$

$$
\triangleq \frac{C(1-\rho_{SR}^2)(\beta\rho_{RD}^2+\rho_{SR}^2(1-(1+\beta)\rho_{RD}^2))}{2b\eta(1-\rho_{RD}^2)(\beta\rho_{RD}^2+\rho_{SR}^2(1-\rho_{RD}^2))}, \tag{20}
$$

$$
\mathcal{A}_{1,RD} \triangleq C\frac{\frac{1}{2\eta b} - \frac{\rho_{SR}^2\left(\frac{b(1-\rho_{RD}^2)}{a(1-\rho_{SR}^2)}\right)^{-1/\rho_{SR}^2}}{2\eta a(\rho_{SR}^2+\beta(1-\rho_{SR}^2)\rho_{RD}^2)}}{1-\frac{\rho_{SR}^2(1-\rho_{RD}^2)\left(\frac{b(1-\rho_{RD}^2)}{a(1-\rho_{SR}^2)}\right)^{1-1/\rho_{SR}^2}}{\beta\rho_{RD}^2+\rho_{SR}^2(1-(1+\beta)\rho_{RD}^2)}}, \tag{21}
$$

$$
\mathcal{A}_{2,SR} \triangleq C\frac{\frac{1}{2a\eta} - \frac{\beta\rho_{RD}^2\left(\frac{a(1-\rho_{SR}^2)}{b(1-\rho_{RD}^2)}\right)^{(-1+\rho_{RD}^2)/\beta\rho_{RD}^2}}{2a\eta(\rho_{SR}^2+(\beta-\rho_{SR}^2)\rho_{RD}^2)}}{1-\frac{\beta(1-\rho_{SR}^2)\rho_{RD}^2\left(\frac{a(1-\rho_{SR}^2)}{b(1-\rho_{RD}^2)}\right)^{(-1+\rho_{RD}^2)/\beta\rho_{RD}^2}}{\beta\rho_{RD}^2+\rho_{SR}^2(1-(1+\beta)\rho_{RD}^2)}}, \tag{22}
$$

and $\mathcal{A}_{2,RD} \triangleq$

$$
C\frac{\left(\frac{a(1-\rho_{SR}^2)}{b(1-\rho_{RD}^2)}\right)^{-1/\beta}(\beta\rho_{RD}^2+\rho_{SR}^2(1-(1+\beta)\rho_{RD}^2))}{2\eta b(\beta\rho_{RD}^2+\rho_{SR}^2(1-\beta\rho_{RD}^2))}. \tag{23}
$$

Proof: Please refer to the Appendix C. ■

The error rate expressions for both Cases a and b are in closed form and can be readily evaluated. Following Corollary 1, we can easily obtain the diversity and coding gains for both cases. We note that for both cases in Protocol 2, perfect CSI yields the same error rate as Protocol 1, as expected, and a diversity gain of two. Note that for perfect CSI, the conditional error rate of the links is simply given by a Q–function, as shown in (3), and, the rule in (4) holds.

[7]From (9), we observe that the log term is positive (negative) for Case 1 (Case 2). Hence, the integration regions for $\hat{\gamma}_{SR}$ and $\hat{\gamma}_{RD}$ are quite different for the two cases.

IV. Delay Analysis

In this section, we derive a closed–form expression for the average delay of the considered buffer–aided relaying scheme, which is valid for both protocols. In Fig. 2, we show the state transition diagram for the queue operation at the relay for a buffer of size L. P_{RD} and P_{SR} denote the probabilities of selecting the $R \to D$ and the $S \to R$ links, respectively, and $P_{RD} = 1-P_{SR}$ holds. For convenience, we assume $S_0 = R_0 = 1$ in this section. If the buffer is empty (full), the source (relay) does not transmit, unlike the operation in [20]. The arrival and departure rates are given by $A = (1-P_{RD})(1-P_{\text{full}})$ and $D = P_{RD}(1-P_{\text{empty}})$, respectively, where P_{full} and P_{empty} denote the probabilities of full and empty buffer, respectively. The expressions for P_{SR}, P_{RD}, P_{full}, and P_{empty} will be provided later.

In [8] and [20], the average delay of link selection schemes for fixed–rate transmission was defined as the average time it takes for a symbol to be received at the destination, once the symbol was transmitted by the source. For the proposed protocols, we may observe silent time slots depending on the status of the buffer. The silent time slots, when no successful transmission occurs, also contribute to the end–to–end delay. These events account for the cases when the $R \to D$ link is chosen while the buffer is empty, or the $S \to R$ link is chosen when the buffer is full, so no successful transmission takes place. In this work, we consider for the delay the time it takes for a symbol that awaits transmission at the source until it is received at the destination. Hence, we take into account both the queueing delay and the delay due to silent time slots to compute the average system delay T.

A. Queueing Delay

In the following proposition, we derive the queueing delay T_Q for the considered buffer operation.

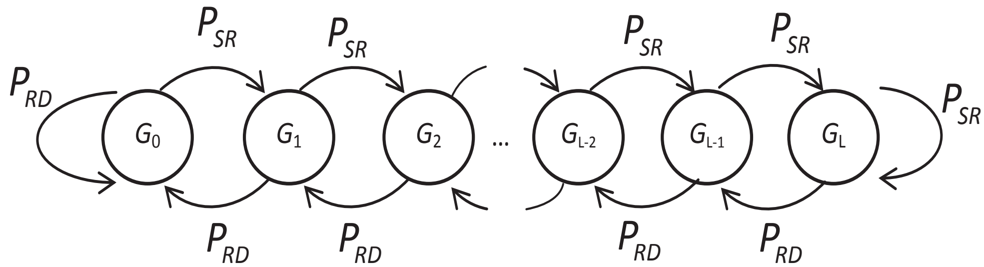

Fig. 2. State transition diagram for queue operation.

Proposition 4: For the considered protocols, the average queueing delay for a buffer of size L is given by

$$T_Q = \frac{L(1-P_{RD})^L(2P_{RD}-1)+P_{RD}((1-P_{RD})^L - P_{RD}^L)}{P_{RD}(2P_{RD}-1)((1-P_{RD})^L - P_{RD}^L)}. \tag{24}$$

and for $L \to \infty$,

$$T_Q = \frac{1}{2P_{RD}-1}, \tag{25}$$

where P_{RD} is the probability of selecting the $R \to D$ link.

Proof: Following the Appendix of [20], we can easily derive the steady state probability of the buffer being in state G_i, denoted by P_{G_i}, $i \in \{0,\ldots,L\}$, cf. Fig. 2. The average queueing delay T_Q of the queue is given by

$$T_Q = \frac{\mathcal{E}\{Q\}}{A}, \tag{26}$$

where the average queue size, $\mathcal{E}\{Q\} = \sum_i iP_{G_i}$, after some manipulations, is obtained as $\mathcal{E}\{Q\}$

$$= \frac{1-P_{RD}}{2P_{RD}-1}\frac{P_{RD}^{L+1}-(1-P_{RD})^L(L(2P_{RD}-1)+P_{RD})}{P_{RD}^{L+1}-(1-P_{RD})^{L+1}}, \tag{27}$$

and $A = (1-P_{RD})(1-P_{\text{full}})$, where $P_{\text{full}} = P_{G_L}$ denotes the probability of observing a full buffer and is given by

$$P_{\text{full}} = \frac{(2P_{RD}-1)(1-P_{RD})^L}{P_{RD}^{L+1}-(1-P_{RD})^{L+1}}. \tag{28}$$

We use P_{full} to calculate A, which we substitute, along with $\mathcal{E}\{Q\}$ from (27), into (26) to obtain the expression shown in (24). For $L \to \infty$, $P_{\text{full}} \to 0$ holds and we obtain the average delay as shown in (25). ■

Remark 7: From (25), we observe that as $P_{RD} \to 1$ (i.e., the departure rate is very high), T_Q approaches the minimum value of one, i.e., on average a packet experiences a queueing delay of one time slot only. On the other hand, when $P_{RD} \to \frac{1}{2}^+$ (i.e., when $P_{RD} \to P_{SR}$), a large queueing delay results. This is because departure rate and arrival rate are nearly equal which causes a packet to be held in the buffer for a large number of time slots. In general, for infinite buffer size, we need $P_{RD} \geq P_{SR}$ to ensure that the buffer is stable[8].

B. Silent Time Slots

Note that for finite buffer size, the probability that the buffer is full or empty is not zero. According to our protocol, we do not force the source (relay) to transmit if the buffer is empty (full), which in turn results in silent time slots, i.e., no transmission takes place. Hence, the number of silent time slots increases as P_{empty} and P_{full} grow. There are two cases when a silent time slot is observed: Case 1) the buffer is full and the $S \to R$ link is selected, and Case 2) the buffer is empty and the $R \to D$ link is selected. Note that Case 1 contributes to the queueing delay, however Case 2 does not. Hence, the delay incurred for Case 2 has to be computed separately. In the following proposition, we provide an expression for the average delay due to observing silent time slots T_S for Case 2.

Proposition 5: For the considered protocols, the average delay due to observing silent time slots for Case 2, i.e., the buffer is empty and the $R \to D$ link is selected, is given by

$$T_S = \frac{(2P_{RD}-1)P_{RD}^L}{(1-P_{RD})(P_{RD}^L-(1-P_{RD})^L)} \tag{29}$$

and for $L \to \infty$,

$$T_S = \frac{2P_{RD}-1}{1-P_{RD}}. \tag{30}$$

Proof: For the considered queue operation, P_{empty} is given by

$$P_{\text{empty}} = P_{G_0} = \frac{P_{RD}^L(2P_{RD}-1)}{P_{RD}^{L+1}-(1-P_{RD})^{L+1}}, \tag{31}$$

and for $L \to \infty$, we obtain

$$P_{\text{empty}} = 2 - \frac{1}{P_{RD}}. \tag{32}$$

For $P_{RD} \to \frac{1}{2}^+$ and $L \to \infty$, we note that $P_{\text{empty}} \to 0$. This is expected as both the links are selected with equal probability and the buffer almost always contains packets in steady state. On the other hand, if $P_{RD} \to 1^-$, the buffer would be empty most of the time as the departure rate is very high, which in turn results in a large number of unused time slots. We consider a sequence of the buffer statuses $\{\text{empty},\ \text{empty},\ \ldots,\text{empty},\text{not empty}\}$, where we want to calculate the average number of time slots the buffer remains empty before R receives a packet. Here, the number of time slots the buffer remains empty before S transmits follows a geometric distribution with mean value $P_{\text{empty}}/(1-P_{\text{empty}})$ [26].

Plugging in the values for $P_{G_0} = P_{\text{empty}}$ from (31), we obtain the expression for T_S in (29). For $L \to \infty$, T_S in (30) is easily obtained after plugging in P_{empty} from (32). ■

Remark 8: For $P_{RD} \to \frac{1}{2}^+$, we note that $T_S \to 0$, as expected. On the other hand, for $P_{RD} > P_{SR}$, T_S increases as the probability of observing silent time slots increases. Note that when $L \to \infty$, silent time slots only occur when the buffer is empty, as $P_{\text{full}} = 0$ for any $P_{RD} > \frac{1}{2}$.

[8]For $S_0 \neq R_0$, we require $R_0P_{RD} > S_0P_{SR}$ to ensure that the buffer is stable. Furthermore, the arrival and departure rates are given by $A = S_0(1-P_{RD})(1-P_{\text{full}})$ and $D = R_0P_{RD}(1-P_{\text{empty}})$, respectively, and the state probabilities P_{G_i} depend on S_0 and R_0 as well.

Corollary 2: For a buffer of size L, the average system delay T in time slots[9] is given by $T = T_Q + T_S$

$$= \frac{L(1-P_{RD})^L(2P_{RD}-1) + P_{RD}((1-P_{RD})^L - P_{RD}^L)}{P_{RD}(2P_{RD}-1)((1-P_{RD})^L - P_{RD}^L)} + \frac{(2P_{RD}-1)P_{RD}^L}{(1-P_{RD})(P_{RD}^L - (1-P_{RD})^L)} \quad (33)$$

and for $L \to \infty$, $T = T_Q + T_S$

$$= \frac{1}{2P_{RD}-1} + \frac{2P_{RD}-1}{1-P_{RD}} = \frac{2-5P_{RD}+4P_{RD}^2}{(1-P_{RD})(2P_{RD}-1)}. \quad (34)$$

Proof: By combining the expressions for T_Q and T_S from Propositions 4 and 5, we can easily obtain T as shown in (33) and (34). ■

To calculate the delay in (33) and (34), we obtain appropriate values for P_{RD} according to the chosen protocol in the following corollary.

Corollary 3: For Protocol 1, P_{RD} is given by

$$P_{RD} = \frac{\beta\bar{\gamma}_{RD}}{(\bar{\gamma}_{SR} + \beta\bar{\gamma}_{RD})}, \quad (35)$$

and for Protocol 2, P_{RD} is given by

$$P_{RD} = \begin{cases} 1 - \frac{\left(\frac{\mu_{RD}}{\mu_{SR}}\right)^{1-1/\rho_{SR}^2} \rho_{SR}^2(1-\rho_{RD}^2)}{\beta\rho_{RD}^2 + \rho_{SR}^2(1-(1+\beta)\rho_{RD}^2)}, & \text{Case } a \\ \frac{\beta\left(\frac{\mu_{SR}}{\mu_{RD}}\right)^{(-1+\rho_{RD}^2)/\beta\rho_{RD}^2}(1-\rho_{SR}^2)\rho_{RD}^2}{\beta\rho_{RD}^2 + \rho_{SR}^2(1-(1+\beta)\rho_{RD}^2)}, & \text{Case } b \end{cases} \quad (36)$$

Proof: For Protocol 1, we calculate $P_{RD} = 1 - P_{SR}$ in (35) by using (74). For protocol 2, Case *a*, $P_{RD} = \Pr(\hat{\gamma}_{SR} < l_1)$ is obtained from (82). Following a similar approach as for Case *a* (cf. Appendix C), the expression for $P_{RD} = \Pr(\hat{\gamma}_{RD} > l_2)$ shown in (36) can be obtained for Case *b*. ■

Combining (33) and (34) with (35) and (36), we obtain closed–form expressions for the average delays for both finite and infinite buffer sizes for both protocols. For example, for Protocol 1, we obtain a simple expression for the average delay for infinite buffer size as

$$T = -\frac{2\bar{\gamma}_{SR}^2 - \beta\bar{\gamma}_{SR}\bar{\gamma}_{RD} + \beta^2\bar{\gamma}_{RD}^2}{\bar{\gamma}_{SR}^2 - \beta\bar{\gamma}_{SR}\bar{\gamma}_{RD}}, \quad (37)$$

where we use (34) and P_{RD} from (35).

In Section VI, we discuss the choice of β and how delay depends on P_{RD} and β for both protocols and also focus on optimization of the error rate for a target delay constraint.

Remark 9: As P_{SR} and P_{RD} are not affected by outdated CSI[10] in Protocol 1, the average delay in (37) holds for all values of ρ_{SR} and ρ_{RD}. However, the delay for Protocol 2 depends on ρ_{AB}, $AB \in \{SR, RD\}$, which stems from the fact that the link selection probabilities $P_{SR} = 1 - P_{RD}$ and P_{RD} are functions of ρ_{AB}, cf. (36).

Remark 10: We note that reordering the queue at the buffer to give priority to individual packets does not affect the average delay. In particular, if the queue is reordered, the total number of packets remaining in the queue does not change and the average queue size remains unchanged. As the arrival rate is also unaffected by this, the average delay expressions presented in this section are still valid, but the delivery of individual packets will be faster or slower due to the reordering, of course.

V. Throughput Analysis

In this section, we investigate the achievable throughput for the proposed link selection protocols. It is obvious that we achieve the maximum throughput when silent time slots are avoided. This can be achieved when both links are selected with equal probability. We denote this throughput as τ_0. However, in practice, we may want to choose β such that the $R \to D$ link is selected more often than the $S \to R$ link in order to achieve a finite delay, which in turn results in some silent time slots. These silent time slots constitute outage events[11] which lower the system throughout. The throughput in the presence of silent time slots is denoted as τ and is given by

$$\tau = \tau_0(1 - F_{\text{silent}}), \quad (38)$$

where F_{silent} denotes the probability of observing a silent time lot. For finite buffer size, we have $F_{\text{silent}} = P_{\text{empty}}P_{RD} + P_{\text{full}}P_{SR}$, whereas for infinite buffer size, $F_{\text{silent}} = P_{\text{empty}}P_{RD}$. Recall from Section IV-B that $A = P_{SR}(1-P_{\text{full}})R_0$ and $D = P_{RD}(1-P_{\text{empty}})R_0$. The maximum throughput[12] $\tau_0 = R_0/2$ can be achieved for infinite buffer size if there are no silent time slots and both links are selected with equal probability, i.e., $P_{RD} = P_{SR}$. Below, we calculate the throughput for the two proposed protocols for both finite and infinite buffer sizes.

For a buffer of finite size, we obtain from (28), (31), (38)

$$\begin{aligned} \tau &= \tau_0(1 - P_{\text{empty}}P_{RD} - P_{\text{full}}P_{SR}) \\ &= \tau_0 \frac{2(1-P_{RD})P_{RD}(P_{RD}^L - (1-P_{RD})^L)}{(1-P_{RD})^L P_{RD} + P_{RD}^{L+1} - (1-P_{RD})^L} \end{aligned} \quad (39)$$

where we use $P_{SR} = 1 - P_{RD}$. Note that $\tau = A$ holds as well and (39) can also be obtained from

$$\begin{aligned} \tau &= R_0(1-P_{RD})(1-P_{\text{full}}) \\ &= 2\tau_0(1-P_{RD})\left(1 - \frac{(2P_{RD}-1)(1-P_{RD})^L}{P_{RD}^{L+1} - (1-P_{RD})^{L+1}}\right). \end{aligned} \quad (40)$$

For a buffer of infinite size, we obtain from (32), (38), (39),

$$\tau = \tau_0(1 - P_{\text{empty}}P_{RD}) = 2\tau_0(1-P_{RD}), \quad \text{when} \quad P_{RD} \geq \frac{1}{2}, \quad (41)$$

or, $\tau = A = R_0 P_{SR} = 2\tau_0(1 - P_{RD})$, as $P_{\text{full}} = 0$ when $L \to \infty$.

Remark 11: The maximum achievable throughput for finite buffer size is less than that for infinite buffer size. We observe that for $P_{RD} = 1/2$, we have $\tau = \tau_0$ ($P_{\text{empty}} = 0$ holds when $P_{RD} = 1/2$) in (41), whereas $P_{\text{empty}}P_{RD} + P_{\text{full}}P_{SR}$ in (39) is never zero for any value of P_{RD}. This also relates to the fact that we strictly need $P_{RD} \geq 1/2$ for infinite buffer size to ensure stability, whereas finite size buffers are never unstable.

[9] Note that we assume that the queueing at the buffer and silent time slots are the dominant sources of packet delay for the considered protocol, and other forms of delay such as transmission delay are negligible.

[10] Recall that the actual and the outdated CSI follow the same distribution.

[11] Here, an outage event corresponds to no transmission, i.e., an unused time slot.

[12] We note that for $S_0 \neq R_0$, the maximum throughput is given by $\tau_0 = S_0 R_0/(S_0 + R_0)$.

$$\tau=\tau_0\frac{2\beta\bar{\gamma}_{RD}\left(1-\frac{\beta\bar{\gamma}_{RD}}{\bar{\gamma}_{SR}+\beta\bar{\gamma}_{RD}}\right)\left(\left(\frac{\beta\bar{\gamma}_{RD}}{\bar{\gamma}_{SR}+\beta\bar{\gamma}_{RD}}\right)^L-\left(1-\frac{\beta\bar{\gamma}_{RD}}{\bar{\gamma}_{SR}+\beta\bar{\gamma}_{RD}}\right)^L\right)}{(\bar{\gamma}_{SR}+\beta\bar{\gamma}_{RD})\left(\left(\frac{\beta\bar{\gamma}_{RD}}{\bar{\gamma}_{SR}+\beta\bar{\gamma}_{RD}}\right)^{L+1}-\left(1-\frac{\beta\bar{\gamma}_{RD}}{\bar{\gamma}_{SR}+\beta\bar{\gamma}_{RD}}\right)^L+\frac{\beta\bar{\gamma}_{RD}\left(1-\frac{\beta\bar{\gamma}_{RD}}{\bar{\gamma}_{SR}+\beta\bar{\gamma}_{RD}}\right)^L}{\bar{\gamma}_{SR}+\beta\bar{\gamma}_{RD}}\right)}, \tag{42}$$

From (41), we observe that throughput monotonically decreases as P_{RD} increases from $1/2$ to 1. From Remark 4, we can intuitively observe that throughput decreases if β increases in the region $P_{RD}>\frac{1}{2}$. Below, we discuss the achievable throughput for the two proposed protocols and also compute the decision threshold β to achieve maximum throughput τ_0. For Protocol 2 and finite buffer size, we do not show the final closed–form throughput for brevity, but the expression can be easily obtained using (39) and substituting P_{RD}. We provide the expressions for infinite buffer sizes for both cases.

A. Protocol 1

In the following corollary, we obtain end–to–end average throughput for Protocol 1.

Corollary 4: For Protocol 1, throughput τ for buffer size L is given by (42) and for $L\to\infty$

$$\tau=\tau_0\frac{2\bar{\gamma}_{SR}}{\bar{\gamma}_{SR}+\beta\bar{\gamma}_{RD}}. \tag{43}$$

Proof: Using (39), (41), and P_{RD} from (35), we obtain τ as shown in (42) and (43). We need $\beta\geq\bar{\gamma}_{SR}/\bar{\gamma}_{RD}$ in (43) to ensure buffer stability and $\beta=\bar{\gamma}_{SR}/\bar{\gamma}_{RD}$ yields maximum throughput τ_0. For finite buffer size, the value of β, which minimizes $P_{\text{empty}}P_{RD}+P_{\text{full}}P_{SR}$, also maximizes τ in (42) and is obtained numerically. ■

B. Protocol 2

For Protocol 2, the end–to–end throughput for infinite buffer size is provided in the following corollary.

Corollary 5: For Protocol 2, throughput τ for $L\to\infty$ and $P_{RD}\geq 1/2$ is given by $\tau=$

$$\begin{cases}2\tau_0\left(\frac{\left(\frac{\mu_{RD}}{\mu_{SR}}\right)^{1-1/\rho_{SR}^2}\rho_{SR}^2(1-\rho_{RD}^2)}{\beta\rho_{RD}^2+\rho_{SR}^2(1-(1+\beta)\rho_{RD}^2)}\right), \text{Case } a\\ 2\tau_0\left(1-\frac{\beta\left(\frac{\mu_{SR}}{\mu_{RD}}\right)^{(-1+\rho_{RD}^2)/\beta\rho_{RD}^2}(1-\rho_{SR}^2)\rho_{RD}^2}{\beta\rho_{RD}^2+\rho_{SR}^2(1-(1+\beta)\rho_{RD}^2)}\right), \text{Case } b\end{cases} \tag{44}$$

Proof: Combining (36) and (41), we obtain the expressions of τ for both cases, as shown in (44). From (36), we solve $P_{RD}=1/2$ for β for Case a and obtain $\beta=l_3$ which yields $\tau=\tau_0$, where l_3 is given by

$$l_3\triangleq\frac{\left(2\left(\frac{\mu_{RD}}{\mu_{SR}}\right)^{1-1/\rho_{SR}^2}-1\right)\rho_{SR}^2(1-\rho_{RD}^2)}{\rho_{RD}^2(1-\rho_{SR}^2)}. \tag{45}$$

Here, $\beta\geq l_3$ ensures a stable buffer operation. For Case b, P_{RD} in (36) is non–linear in β. Hence, β is obtained numerically for $P_{RD}\geq 1/2$. ■

Remark 12: From (42)–(44), we observe that for Protocol 1, the throughput does not depend on the reliability of the CSI estimates, ρ_{AB}, $AB\in\{SR,RD\}$. However, for Protocol 2, it does.

As a special case, we obtain the achievable throughput for perfect CSI and infinite buffer size by replacing $\rho_{AB}=1$ in (44)

$$\tau=\tau_0\frac{2\bar{\gamma}_{SR}}{\bar{\gamma}_{SR}+\beta\bar{\gamma}_{RD}}. \tag{46}$$

As expected, the throughput for perfect CSI is identical to (43), i.e., the throughput of Protocol 1. This is because both actual and outdated CSI follow the same distribution.

VI. Trade–off and Choices for β

The parameter β has to be properly chosen to maintain buffer stability and to obtain a trade–off among three relevant performance metrics: error rate, delay, and throughput. In this section, we study the dependence of the error rate, delay, and throughput on β in detail [13]. First, we discuss the convexity and/or monotonicity of the performance metrics w.r.t. β, which will be useful later when we optimize the error rate by tuning β under delay and throughput constraints.

A. SER vs. β

For both protocols, $P(e)$ is in general not convex in β, except for $\rho_{SR}=\rho_{RD}=1$ and high SNR[14]. The value of β which yields minimum SER is not necessarily the same for both protocols. Below, we discuss special cases when $\beta=1$ results in the minimum SER.

Corollary 6: For perfect CSI, i.e., when $\rho_{AB}=1$, $\beta=1$ results in minimum SER at high SNR.

Proof: For $\bar{\gamma}_{SR}=a\bar{\gamma}$, $\bar{\gamma}_{RD}=b\bar{\gamma}$, $\bar{\gamma}\to\infty$, where a and b are positive constants, the asymptotic expression for $P(e)$ when $\rho_{AB}=1$ is provided in (14). Taking the first derivative of $P(e)$ w.r.t. β yields

$$\frac{dP(e)}{d\beta}=\frac{3C\left(\beta^2-1\right)}{4ab\beta^2\bar{\gamma}^2\eta^2}. \tag{47}$$

Solving $\frac{dP(e)}{d\beta}=0$, we obtain $\beta=\{1,-1\}$. As $\beta=-1$ is not feasible, $\beta=1$ holds. ■

Corollary 7: For symmetric links, i.e., $\rho_{SR}=\rho_{RD}=\rho$ and $\bar{\gamma}_{SR}=\bar{\gamma}_{RD}$, $\beta=1$ results in minimum SER for both protocols.

Proof: For $\bar{\gamma}_{SR}=\bar{\gamma}_{RD}=\bar{\gamma}$, and $\rho_{SR}=\rho_{RD}=\rho$, i.e., $\mu_{SR}=\mu_{RD}=\mu$, the expressions for $P(e)$ in (18) are identical for both cases. Taking the first derivative of $P(e)$ of Case a in (18) w.r.t. β yields

$$\frac{dP(e)}{d\beta}=\frac{(\beta^2-1)\rho^4(2-\rho^2)(1-\rho^2)^2}{\mu(1+\beta-\rho^2)^2(-1+\beta(-1+\rho^2))^2}. \tag{48}$$

[13]The choice of β is also affected by the transmission rates S_0 and R_0, if they are unequal. As mentioned in Section II, in this paper, we assume identical transmission rates and focus on how the optimal β is affected by the channel fading statistics.

[14]From (14), for $\rho_{SR}=\rho_{RD}=1$ we obtain $P_e=\frac{3C}{4\eta^2\bar{\gamma}^2}(\frac{a^2+b^2}{ab}+\frac{1}{\beta ab}+\frac{\beta}{ab})$, where the sum inside the parenthesis is convex in $\beta\in\mathbb{R}^+$.

Solving $\frac{dP(e)}{d\beta} = 0$, we obtain $\beta = \{1, -1\}$. As $\beta = -1$ is not feasible, $\beta = 1$ holds. Using (13), similar results can be obtained for Protocol 1. ■

We can intuitively justify Corollary 7 as follows: The link selection criterion for symmetric links is given by (11). $\beta = 1$ means that the link will be selected based on the instantaneous CSI only, i.e., the link is selected based on $\max(\hat{\gamma}_{SR}, \hat{\gamma}_{RD})$. Hence, given that the reliabilities of the CSI estimates of the two links are identical, this rule implies that selecting the strongest link in terms of the outdated instantaneous SNR is optimal.

For other cases, we find the β yielding minimum SER for the two protocols numerically. For a particular set of $\bar{\gamma}_{AB}$ and ρ_{AB}, $\forall AB$, the value of β which provides minimum SER can be different for the two protocols. However, note that the value of β, which achieves minimum SER, may not always be a feasible choice because it may incur buffer instability and entail a large delay and/or low throughput.

B. Delay vs. β

In practice, there may be a limit on the tolerable system delay. Unless mentioned otherwise, we assume infinite buffer size in this section and provide some insight on the delay performance of the considered protocols. To ensure buffer stability, we need to operate in the region $P_{RD} \geq 1/2$, which shrinks the search space for the optimal β minimizing the SER. However, from Section IV, we know that $P_{RD} = 1/2$ introduces infinite delay, because both links are selected with equal probability. Below, we examine the behaviour of the average delay as a function of β in the region $P_{RD} > 1/2$. The following proposition holds for both protocols.

Proposition 6: For infinite buffer size, the delay T is convex in P_{RD} for $P_{RD} > 1/2$. A minimum delay of $T_{\min} = 1 + 2\sqrt{2}$ time slots can be observed when $P_{RD} = \frac{1}{\sqrt{2}}$.

Proof: From (34), we obtain

$$\frac{dT}{dP_{RD}} = \frac{2P_{RD}^2 - 1}{(2P_{RD} - 1)^2(1 - P_{RD})^2}, \tag{49}$$

$$\frac{d^2T}{dP_{RD}^2} = \frac{2}{(1 - P_{RD})^3} + \frac{8}{(2P_{RD} - 1)^3}, \tag{50}$$

where $\frac{d^2T}{dP_{RD}^2} \geq 0$, when $P_{RD} \geq \frac{1}{2}$. Hence, T is convex in P_{RD}, when the $R \to D$ link is selected more often than the $S \to R$ link. Furthermore, solving for $dT/dP_{RD} = 0$, we obtain $P_{RD} = 1/\sqrt{2}$ and this results in $T_{\min} = 1 + 2\sqrt{2}$. ■

Furthermore, to obtain a target delay T, we solve for P_{RD} in (34)

$$P_{RD} = \{P_{RD,1}, P_{RD,2}\} = \left\{ \frac{5 + 3T - \sqrt{T^2 - 2T - 7}}{4(T + 2)}, \frac{5 + 3T + \sqrt{T^2 - 2T - 7}}{4(T + 2)} \right\}. \tag{51}$$

Note that $P_{RD,1} \leq 1/\sqrt{2} \leq P_{RD,2}$ holds and both values of P_{RD} are valid since both $\{P_{RD,1}, P_{RD,2}\}$ ensure buffer stability, i.e., they are larger than $1/2$ because in (51)

$$\lim_{T \to \infty} \frac{5 + 3T - \sqrt{T^2 - 2T - 7}}{4(T + 2)} = \frac{1}{2} \tag{52}$$

holds.

Next, we study the delay as a function of β. It is difficult, if not impossible, to analytically prove the convexity or quasi–convexity of T (cf. (33)) in β and obtain a closed–form solution for β for any buffer size L. However for some special cases, we can prove the convexity of the delay for the two protocols, as discussed in the following propositions. We also calculate the value of β which yields minimum delay. For Protocol 2, we only show results for Case *a* because in Case *b*, P_{RD} is highly non–linear in β, and it is difficult to prove convexity of the delay in β or solve for β analytically to achieve a target delay.

Proposition 7: For infinite buffer size, delay T is convex in β for $\beta > \bar{\gamma}_{SR}/\bar{\gamma}_{RD}$ in Protocol 1 and for $\beta > \frac{2d-c}{g}$ in Protocol 2 Case *a*, where $\{c, d, g\}$ are positive constants and defined as

$$c \triangleq \rho_{SR}^2(1 - \rho_{RD}^2),\ d \triangleq \left(\frac{\mu_{RD}}{\mu_{SR}}\right)^{1 - \frac{1}{\rho_{SR}^2}} \rho_{SR}^2(1 - \rho_{RD}^2),$$
$$g \triangleq \rho_{RD}^2(1 - \rho_{SR}^2). \tag{53}$$

Furthermore, $\beta = (1 + \sqrt{2})\xi$, where $\xi \triangleq \bar{\gamma}_{SR}/\bar{\gamma}_{RD} \in \mathbb{R}^+$ and $\beta = \frac{(2+\sqrt{2})d - c}{g}$ results in a minimum delay of $T_{\min} = 1 + 2\sqrt{2}$ time slots for Protocol 1 and Protocol 2 Case *a*, respectively.

Proof: From (37), we obtain

$$T = \frac{\beta}{\xi} + \frac{2\xi}{-\xi + \beta}, \tag{54}$$

where the r.h.s. of (54) is convex[15] in β only if $\beta > \xi$. On the other hand, P_{RD} for Protocol 2 Case *a* is given by (36), which can be simplified as

$$P_{RD} = 1 - \frac{d}{c + g\beta}, \tag{55}$$

where $\{c, d, g\}$ are defined above. Now, delay T in (34) can be expressed as

$$T = \frac{c - d}{d} + \frac{g\beta}{2d} + \frac{2d}{-2d + c + g\beta}, \tag{56}$$

where, using a similar argument as for Protocol 1, the r.h.s. of (56) is convex in β only if $\beta > \frac{2d-c}{g}$. Furthermore, calculating $dT/d\beta = 0$ from (54) and (56), we obtain $\beta^* = (1 + \sqrt{2})\xi$ and $\beta^* = \frac{(2+\sqrt{2})d - c}{g}$ for Protocol 1 and Protocol 2 Case *a*, respectively, which satisfy the condition $d^2T/d\beta^2|_{\beta=\beta^*} > 0$. Plugging in β^* into T, we obtain $T_{\min} = 1 + 2\sqrt{2}$ time slots. ■

Note that both $\beta > \xi$ and $\beta > \frac{2d-c}{g}$ in Proposition 7 correspond to $P_{RD} > 1/2$. Recall from Section II that P_{RD} monotonically increases with β. Exploiting Proposition 6, we can calculate the value of β corresponding to $P_{RD,1}$ and $P_{RD,2}$ to achieve a target delay T for both protocols by using appropriate expressions of P_{RD} as function of β (cf. Corollary 3 where P_{RD} is shown as a function of β). We refer to them

[15]Note that $r/(s + x)$ is convex in x for $r > 0$ and $x \in (-s, \infty)$.

as β_1 and β_2. For Protocol 1, we obtain $\beta =$

$$\Big\{ \underbrace{\frac{\xi}{2}(T+1+\sqrt{-7-2T+T^2})}_{\beta_1}, \underbrace{\frac{\xi}{2}(T+1-\sqrt{-7-2T+T^2})}_{\beta_2} \Big\}, \tag{57}$$

$$\text{where} \qquad \beta_1, \beta_2 > \xi, \quad \text{as} \quad T > \sqrt{-7-2T+T^2}. \tag{58}$$

Similarly, for Protocol 2 Case a, we obtain $\beta =$

$$\Bigg\{ \underbrace{\frac{-c+d+d(T-\sqrt{-3-2T+T^2})}{g}}_{\beta_1}, \underbrace{\frac{-c+d+d(T+\sqrt{-3-2T+T^2})}{g}}_{\beta_2} \Bigg\}, \tag{59}$$

where

$$\beta_1, \beta_2 > \frac{2d-c}{g}, \quad \text{as} \quad T > \sqrt{-3-2T+T^2}. \tag{60}$$

Remark 13: Both β_1 and β_2 in (58) and (60) ensure stable buffer operation and $\beta_1 \leq \beta^* \leq \beta_2$ holds. The intuitive reason for having two solutions for the same delay is because as $P_{RD} \to \frac{1}{2}^+$, i.e., $\beta \to \xi^+$ for Protocol 1 or $\beta \to \frac{2d-c}{g}$ for Protocol 2 Case a ($P_{RD} \to 1^-$, i.e., $\beta \gg \xi$ (Protocol 1) or $\beta \gg \frac{2d-c}{g}$ for Protocol 2 Case a, T_Q increases and T_S decreases (and vice–versa). This inverse behaviour of the two delay components with respect to β also explains why an average system delay below a certain value, i.e., $T_{\min} = 1+2\sqrt{2}$ in our case, is not possible.

Next, in the following Proposition, we focus on $L = 1$ as a special of the finite buffer size.

Proposition 8: For $L = 1$, the delay is convex in $\beta \in \mathbb{R}^+$ for Protocol 1 and in $\beta > \frac{d-c}{g}$ for Protocol 2 Case a. A minimum delay of $T_{\min} = 3$ time slots is achieved when $P_{RD} = \frac{1}{2}$ or $\beta^* = \xi$ (Protocol 1) and $\beta^* = \frac{2d-c}{g}$.

Proof: Substituting $L = 1$ in (33), we obtain

$$T = \frac{1}{P_{RD}} + \frac{P_{RD}}{1-P_{RD}} = \frac{\beta}{\xi} + \frac{\xi}{\beta} + 1, \tag{61}$$

where $P_{RD} = \frac{\beta}{\xi+\beta}$ is used, cf. Corollary 3. Clearly, T is convex in $\beta \in \mathbb{R}^+$. Furthermore, solving $dT/d\beta = 0$, we obtain $\beta = \{-\xi, \xi\}$. Discarding $\beta = -\xi$, we get $d^2T/d\beta^2|_{\beta=\xi} = \frac{2}{\xi^2} > 0$. Hence, $\beta^* = \xi$ or $P_{RD} = \frac{1}{2}$ yields the minimum T. After plugging this value into (61), we obtain $T_{\min} = 3$. Similarly, for Protocol 2 Case a, we obtain

$$T = \frac{c}{d} + \frac{g\beta}{d} + \frac{d}{c-d+g\beta}, \tag{62}$$

where T is convex in β if $\beta > \frac{d-c}{g}$. Following a similar approach as adopted for Protocol 1, we can show that $\beta^* = \frac{2d-c}{g}$ yields the minimum delay of $T_{\min} = 3$. ■

Remark 14: In views of Proposition 7 and 8, we conjecture that the minimum achievable delay increases from three to $1+2\sqrt{2}$, as the buffer size increases from one to ∞. We validate this claim in Section VII.

For other values of L, we obtain β numerically to achieve a target delay. As P_{RD} is a non–linear function of β for Protocol 2 and Case b, cf. (36), it is difficult to obtain a closed–form expression for β. We exploit the monotonicity of P_{RD} in β, cf. Remark 4, and we calculate β_1 and β_2 numerically for a target delay T, by using (36) and (51), for Case b.

C. Throughput vs. β

From (41) in Section V, we observe throughput τ decreases monotonically with P_{RD}, as expected. Note that $P_{RD} = \frac{1}{2}$ yields the maximum throughput τ_0, and as $P_{RD} \to 1^-$, τ approaches zero. Furthermore, considering Remark 4, we conclude that τ monotonically decreases with β.

The following Corollaries provide some insight, regrading the achievable throughput if the end–to–end delay is minimized.

Corollary 8: For infinite buffer size and $T = T_{\min} = 1+2\sqrt{2}$, the achievable throughput is $\tau = (2-\sqrt{2})\tau_0$.

Proof: We observed from Proposition 6 that $P_{RD} = 1/\sqrt{2}$ yields the minimum delay. Plugging $P_{RD} = 1/\sqrt{2}$ into $\tau = \tau_0(2-2P_{RD})$ (cf. (41)), we obtain $\tau = (2-\sqrt{2})\tau_0 = 0.5858\tau_0$. ■

Corollary 9: For $L = 1$ and $T = T_{\min} = 3$, the achievable throughput is $\tau = \tau_0/2$.

Proof: We observed from Proposition 8 that $P_{RD} = 1/2$ yields the minimum delay for $L = 1$. From (39), we obtain $\tau = 2\tau_0(1-P_{RD})P_{RD}$ for $L = 1$. Plugging in $P_{RD} = 1/2$, we obtain $\tau = \tau_0/2$. ■

The values of β corresponding to Corollaries 8 and 9, are derived in Propositions 7 and 8 for Protocol 1 and Protocol 2 Case a, respectively. For Protocol 2 Case b, we calculate β numerically, as indicated before.

Remark 15: From Corollary 9, we observe that for the proposed protocols, the maximum achievable throughput for $L = 1$ is half the value that can be obtained if a buffer of infinite size is employed. In other words, as the buffer size increases, we expect an increase in the throughput.

D. Optimization of SER

In practice, there may be constraints on the minimum achievable throughput and the maximum end–to–end delay. Here, we formulate an optimization problem for β and our objective is to minimize the SER for a maximum allowable delay $T_{\max}$ and a minimum required throughput $\tau_{\min}$, i.e.,

$$\min_{\beta} \quad P(e) \tag{63}$$
$$\text{s.t.} \begin{cases} T \leq T_{\max} \\ \tau \geq \tau_{\min} \end{cases},$$

We cannot adopt tools from convex optimization here, as $P(e)$ is not convex in β in general. However, we perform a simple one–dimensional search over β within the range specified by the delay and throughput constraints, and minimize $P(e)$ over this range. Let $\{\beta_1, \beta_2\}$ yield delay $T = T_{\max}$, where $\beta_2 > \beta_1$ holds, cf. (58), (60). We assume $\beta = \beta_3$ results in $\tau = \tau_{\min}$, cf. (42)–(44) and $\beta = \beta_4$ corresponds to $P_{RD} = 1/2$, i.e., $\tau = \tau_0$. Then, we search in the interval

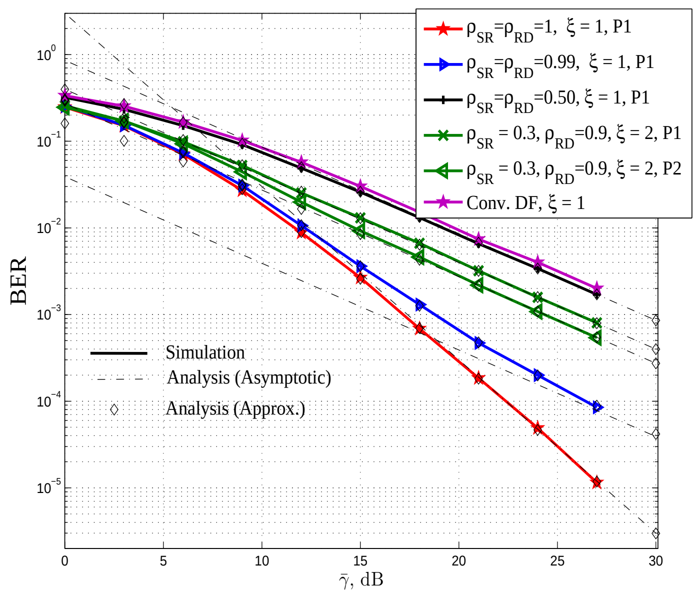

Fig. 3. BER vs. SNR ($\bar{\gamma}$) performance without delay constraints. P1 and P2 refers to Protocol 1 and Protocol 2, respectively.

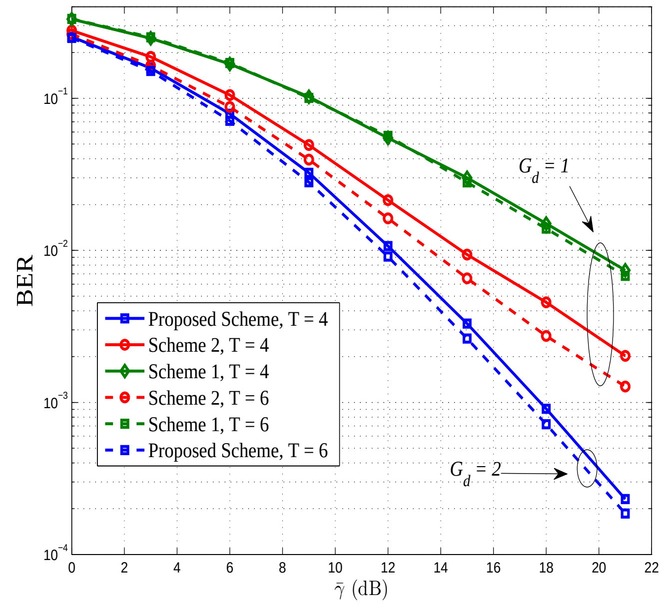

Fig. 4. BER vs. SNR ($\bar{\gamma}$) performance with delay constraints.

$\max\{\beta_4, \beta_1\} \leq \beta \leq \min\{\beta_2, \beta_3\}$. Hence, we transform the problem as

$$\min_{\beta_l \leq \beta \leq \beta_u} \quad P(e), \tag{64}$$

where $\beta_l \triangleq \max\{\beta_4, \beta_1\}$ and $\beta_u \triangleq \min\{\beta_2, \beta_3\}$. If $\beta_3 < \beta_1$, then the delay and throughput constraints cannot be simultaneously satisfied. This could happen when only a very small delay can be afforded ($\{\beta_1, \beta_2\} \rightarrow \beta^*$) while a very high throughput is required ($\beta_3 \rightarrow \beta_4$). For infinite buffer size $\beta_l = \beta_1$ holds as $\beta_1 > \beta_4$ is valid. However, for finite buffer size, we may have $\beta_1 < \beta_4$. Recall from Proposition 8 and Corollary 9 that for $L = 1$, the value of β which yields minimum delay also provides maximum throughput. In view of the discussions above and Section V, we can obtain β_l and β_u analytically for some cases (e.g., infinite buffer size and Protocol 1 or Protocol 2 Case *a*), in other cases, we have to obtain them numerically. In Section VII, we show an example for the considered optimization problem.

VII. Simulation Results

In this section, we illustrate the performance of the link selection schemes for outdated and perfect CSI for the considered three node network. Each node transmits a BPSK modulated ($C = 1$, $\eta = 2$) symbol and the average delay is expressed in time slots, unless otherwise stated. Note that, $\tau_0 = 1/2$ holds for the adopted modulation scheme. We assume equal power allocation $P_S = P_R = P$. First, we study the BER as a function of the transmit SNR $\bar{\gamma} \triangleq P/N_0$ with/without delay constraints and assume $\bar{\gamma}_{RD} = \bar{\gamma}$ and infinite buffer sizes, unless otherwise mentioned. Next, for delay constrained transmission, we investigate the performance of a modified link selection protocol, which aims to improve throughput and delay by allowing threshold–based transmission during silent time slots. Finally, we focus on the dependence of BER, delay, and throughput on β, and constrained BER optimization.

A. BER vs. SNR

In Fig. 3, the BER vs. SNR ($\bar{\gamma}$) is shown when link selection is performed without any delay constraints, i.e., when $P_{RD} = 1/2$ and maximum throughput τ_0 is observed. We consider two values of $\xi = \bar{\gamma}_{SR}/\bar{\gamma}_{RD} \in \{1, 2\}$ in Fig. 3. Here, β is chosen such that $P_{RD} = 1/2$, cf. Section VI. A wide range of values for $\{\rho_{SR}, \rho_{RD}\}$ are considered. We also show the analytical results along with simulation results to corroborate the claims made in Section III. In Fig. 3, "approx." and "asymptotic" refer to (13) and (14) for Protocol 1 and (18) and (19) for Protocol 2. For perfect CSI, we observe a diversity gain of two, as predicted in Section III. When the CSI is outdated, a loss in diversity occurs, and all BER curves for $\rho_{SR}, \rho_{RD} < 1$ exhibit a diversity gain of one at high SNR, similar to conventional (conv.) DF relaying, where the relay receives and transmits in consecutive time slots. A higher coding gain compared to conventional DF relaying is observed for perfect CSI and outdated CSI, especially when the actual and outdated CSI are strongly correlated. We compare Protocol 1 with Protocol 2 for the case when the ρ_{SR} and ρ_{RD} are dissimilar and differ by a large margin, e.g., $\rho_{SR} = 0.3$, $\rho_{RD} = 0.9$. Protocol 2 exploits this dissimilarity by incorporating it into the link selection rule and achieves superior performance (close to 2dB coding gain) compared to Protocol 1 at high SNR.

In Fig. 4, the BER vs. SNR ($\bar{\gamma}$) is shown when link selection is performed for delay constrained transmission. We consider i.i.d. fading here, i.e., $\xi = 1$. β is adjusted to account for the delay constraint, cf. Section VI-B. Here, we assume perfect CSI (i.e., $\rho_{SR} = \rho_{RD} = 1$), and focus on the merits of the proposed protocol in delay constrained transmission compared to other existing buffer–aided relaying protocols for the same average delay. We show here results for $T = \{4, 6\}$ and compare with two existing buffer–aided relaying schemes. In Scheme 1 [5], the relay receives for T time slots, before it transmits for T time slots. In Scheme 2 [20], there is no silent time slots and the source (relay) is forced to transmit if the buffer at the relay

TABLE II

MODIFIED LINK SELECTION PROTOCOL 1 WITH THRESHOLD–BASED TRANSMISSION IN SILENT TIME SLOTS.

Case	Buffer status	Link quality	Selected link
1a	Empty	$\hat{\gamma}_{SR} < \beta\hat{\gamma}_{RD}$ AND $\hat{\gamma}_{SR} > \theta\bar{\gamma}_{SR}$	$S \to R$
1b	Empty	$\hat{\gamma}_{SR} < \beta\hat{\gamma}_{RD}$ AND $\hat{\gamma}_{SR} \le \theta\bar{\gamma}_{SR}$	None
2	Not empty	$\hat{\gamma}_{SR} < \beta\hat{\gamma}_{RD}$	$R \to D$
3a	full	$\hat{\gamma}_{SR} \ge \beta\hat{\gamma}_{RD}$ AND $\hat{\gamma}_{RD} > \phi\bar{\gamma}_{RD}$	$R \to D$
3b	full	$\hat{\gamma}_{SR} \ge \beta\hat{\gamma}_{RD}$ AND $\hat{\gamma}_{RD} \le \phi\bar{\gamma}_{RD}$	None
4	Not full	$\hat{\gamma}_{SR} \ge \beta\hat{\gamma}_{RD}$	$S \to R$

TABLE III

THROUGHPUT AND DELAY OBSERVED WITH DIFFERENT SNR THRESHOLDS. BPSK TRANSMISSION, $\bar{\gamma}_{SR} = 0.2\bar{\gamma}$, $\bar{\gamma}_{RD} = \bar{\gamma}$, AND $\bar{\gamma} = 15$ DB ARE ASSUMED. THE MAXIMUM THROUGHPUT IS $\tau_0 = 0.5$ AND $\xi = 0.2$ IS VALID.

β	SNR threshold θ	Throughput τ	Delay T	BER
0.6	0.1	0.483	2	0.01171
	1	0.355	2.81	0.004
	10	0.251	3.93	0.0032
	∞	0.25	4.0	0.003
1.5	0.1	0.478	1.376	0.01403
	1	0.303	2.545	0.0044
	10	0.117	6.548	0.004
	∞	0.11	7.8	0.004

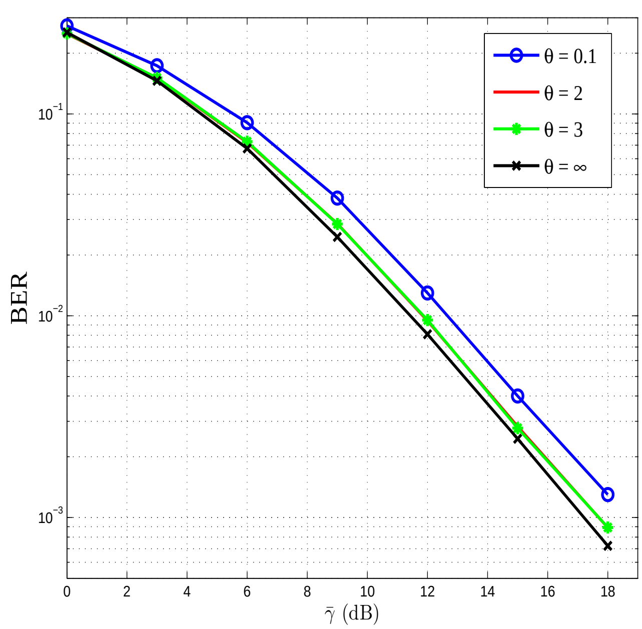

Fig. 5. BER vs. SNR ($\bar{\gamma}$) for different threshold values, $\theta \in \{0.1, 2, 3, \infty\}$. Note that ϕ is not needed here (cf. Table II), as a full buffer cannot occur because of the assumed infinite buffer size.

is empty (full). In Scheme 2, β is calculated using (35) and [20, Eq. (39)]) to achieve a target delay T. Similar to the proposed scheme, the relays in Schemes 1 and 2 forward the detected bits to the destination, regardless of decision errors at the relay. We observe that for both $T = 4$ and $T = 6$, the proposed protocol achieves full diversity, whereas Schemes 1 and 2 achieve a diversity gain of one only, as the best link is not always exploited because of forced transmissions. On the other hand, the proposed scheme suffers from a throughput loss compared to Schemes 1 and 2, where always either the source or the relay transmits and an effective average throughput of $\tau_0 = 1/2$ is achieved, as there are no silent time slots. For $T = 4$, the throughput for the proposed scheme is 66% of τ_0 for $\beta = 2$, whereas for $T = 6$, it increases to 82% of τ_0 for $\beta = 1.44$[16].

B. *Threshold–based Transmission*

Next, we consider a modification of Protocol 1, which allows for a threshold–based transmission during the silent time slots, thus improving throughput and delay at the expense of a degradation of the error rate performance, cf. Table II. In the modified protocol, transmission during a silent time slot is allowed if the outdated instantaneous link SNR is larger than a scalar times the average SNR [17]. A similar modification can be applied for Protocol 2, but is not shown here. We study the case of $\beta > \xi = \bar{\gamma}_{SR}/\bar{\gamma}_{RD}$ (so that silent time slots are observed) and infinite buffer size. θ and ϕ are the scaling parameters in the threshold for the $S \to R$ and $R \to D$ links, respectively, cf. Table II. Hence, $\theta = \phi = \infty$ denotes the original scheme proposed in Section II.

In Fig. 5, we show the simulated BER for different SNR thresholds, $\theta = \{0.1, 2, 3, \infty\}$, for i.i.d. channels, perfect CSI, and adopt $\beta = 2$ and $\xi = 1$. For $\theta = \{2, 3\}$, the BER is slightly worse than for $\theta = \infty$, i.e., no threshold–based transmission during silent time slots. On the other hand, for $\theta = \{2, 3, \infty\}$, throughputs of $\tau = \{0.42, 0.34, 0.33\}$ are observed, i.e., lower

[16]The values of β are obtained from (57). Note that (57) has two solutions for β for achieving a target delay T. We choose the solution for β that yields larger throughput.

[17]We note that alternatively a threshold which is a power of the average SNR could be adopted, i.e., $\gamma_{AB} \ge \bar{\gamma}_{AB}^{c}$, where c is a positive constant. However, this modification does not affect the maximum achievable diversity gain (which is two).

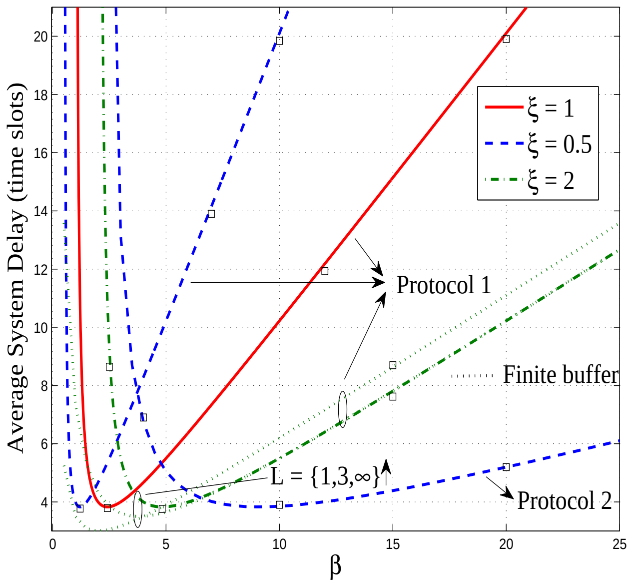

Fig. 6. Average delay vs. β for two protocols. Results are shown for different choices of $\xi = \bar{\gamma}_{SR}/\bar{\gamma}_{RD}$. For $\xi = 0.5$, delay results for Protocol 2 are shown for $\rho_{SR} = 0.9$ and $\rho_{RD} = 0.6$. Delay results for finite buffer sizes $L \in \{1, 3\}$ are shown for Protocol 1, when $\xi = 2$. Square markers denote simulated results.

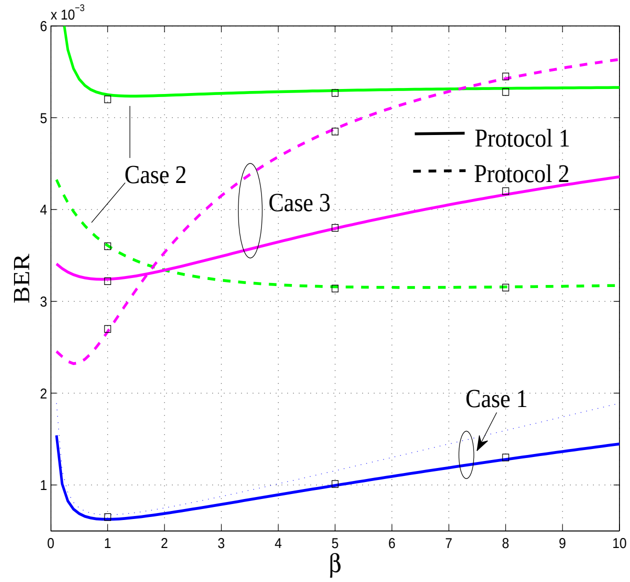

Fig. 7. BER vs. β for the proposed protocols. Case 1) $2\bar{\gamma}_{SR} = \bar{\gamma}_{RD} = 0.5\bar{\gamma}$, $\rho_{SR} = \rho_{RD} = 1$, Case 2) $3\bar{\gamma}_{SR} = \bar{\gamma}_{RD} = 0.75\bar{\gamma}$, $\rho_{SR} = 0.9$, $\rho_{RD} = 0.7$, Case 3) $\bar{\gamma}_{SR} = 2\bar{\gamma}_{RD} = \bar{\gamma}$, $\rho_{SR} = 0.7$, $\rho_{RD} = 0.9$. $\bar{\gamma} = 20$ dB is assumed and square markers denote simulated results.

threshold values yield a higher throughput due to the reduced number of silent time slots at the expense of an increased BER.

This behaviour can also be observed in Table III, where we show the throughput and delay of threshold–based transmission for i.n.d. fading. A lower value of θ implies that S transmits more often when silent time slots are observed due to empty buffers. As θ increases, the delay and throughput performances of the modified protocol approach those of the original scheme. Hence, we conclude from Fig. 5 and Table III that with an appropriate choice of the threshold, improved delay and throughput performances can be achieved for threshold–based transmission at the expense of a small loss in the BER compared to the case where threshold–based transmission is not applied.

C. Performance Trade–offs

In Fig. 6, we show that low average delay can be obtained by the proposed protocols for both finite and infinite buffer sizes. In particular, we show that for both i.i.d. and i.n.d. fading, a delay as low as $1 + 2\sqrt{2} \approx 3.81$ time slots can be observed by choosing β properly for infinite buffer size, as predicted in Section IV. We observe a sharp rise in the average delay when $\beta \to \frac{\bar{\gamma}_{SR}}{\bar{\gamma}_{RD}}$ for infinite buffer size, i.e., T_Q becomes very large. This fact was also alluded to in [20] for the queueing delay. Another interesting observation is that for finite buffer sizes, average delays lower than $1+2\sqrt{2}$ can be achieved, and for $L = 1$, a minimum delay of three time slots is observed, cf. Proposition 8. This result is supported by the fact that the average queueing delay is proportional to the average queue size, which, with appropriate selection of β, can be made smaller for a finite size buffer than for an infinite buffer size. We also note from Fig. 6 that the delay is convex in β over the considered region, as shown in Section VI. Note that the delay vs. β curves shift to the left (right) of that for $\xi = 1$ when $\xi < 1$ ($\xi > 1$). This is because increasing β also increases the probability of selecting the $R \to D$ link (cf. Remark 4) and when the $R \to D$ link is stronger, i.e., $\xi < 1$, we require smaller values of β to achieve a certain delay compared to the cases when $\xi \geq 1$, and vice–versa.

In Fig. 7, we show BER vs. β for both protocols for i.i.d. and i.n.d. links. We consider three cases, as specified in the caption of Fig. 7. We observe that when $\beta = 1$, the lowest BER is achieved for perfect CSI (Case 1), cf. Section VI-A. In other words, when β approaches one (i.e., link selection is performed based on the instantaneous link quality only), the BER performance improves. We also show the asymptotic approximation for the error rate for Case 1 (dotted line) which is convex as claimed in Section VI-A. For i.n.d. fading with dissimilar correlation coefficients, $\beta \neq 1$ yields minimum BER. For Case 2, (9) holds for Protocol 2 which yields better performance compared to Protocol 1. For Case 3, (10) holds for Protocol 2. Note that for some values of β, Protocol 1 results in a lower BER compared to Protocol 2, even though the minimum of the BER for Protocol 2 is lower than that of Protocol 1. However, if we want to compare the BERs of the two protocols for a certain target delay or throughput, different values of β are needed (cf. Remark 5). For example, in Case 3, $\beta = 2$ ($\beta = 0.88$) yields maximum throughput for Protocol 1 (Protocol 2) and $\beta = 3.5$ ($\beta = 1.4$) yields an average delay of $T = 4.41$ time slots for Protocol 1 (Protocol 2). Note that Protocol 2 yields a lower BER for this target delay and throughput. On the other hand, for large delay and/or low throughput, Protocol 1 may yield similar or lower BER compared to Protocol 2. For example, $\beta = 10$ ($\beta = 3.3$) corresponds to 33% of maximum throughput for Protocol 1 (Protocol 2), and both protocols perform similarly in terms of BER.

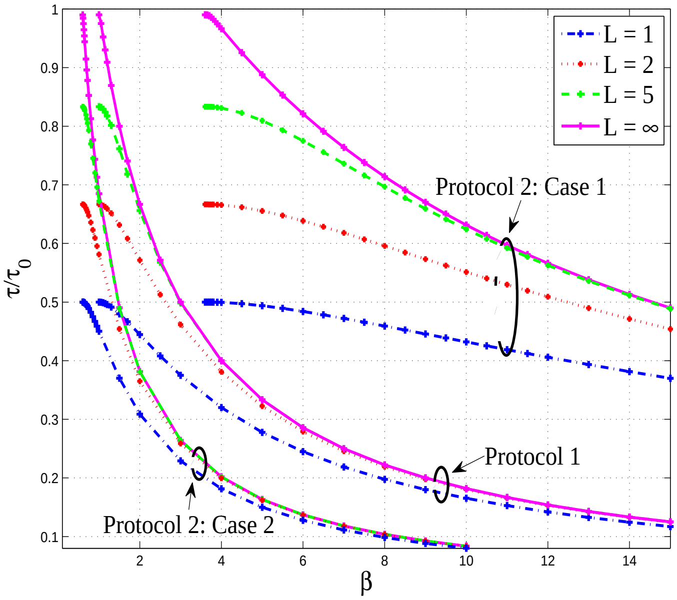

Fig. 8. Normalized throughput vs. β for the two considered protocols for different buffer sizes $L \in \{1, 2, 5, \infty\}$. Protocol 1: $\xi = 1$, Protocol 2 Case *a*: $\xi = 1$, $\rho_{SR} = 0.9$, $\rho_{RD} = 0.6$, Protocol 2 Case *b*: $\xi = 1$, $\rho_{SR} = 0.6$, $\rho_{RD} = 0.9$. $\bar{\gamma} = 20$ dB is assumed.

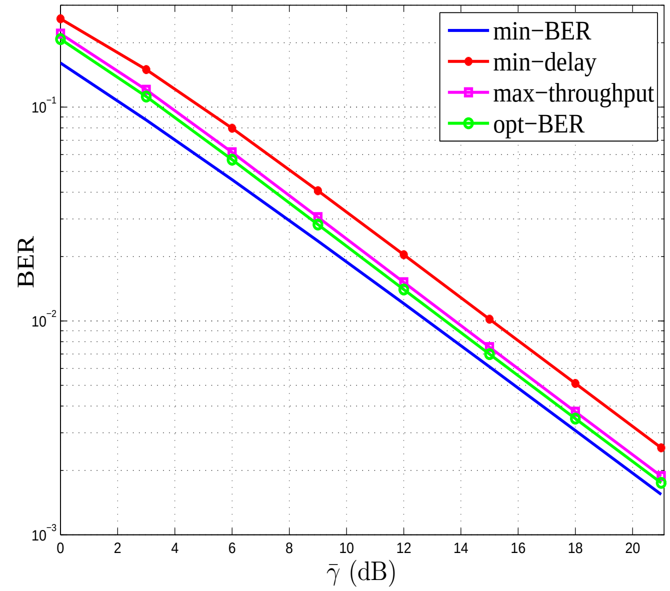

Fig. 9. BER vs. SNR ($\bar{\gamma}$) optimization for infinite buffer size, under different objectives. For min–BER, min–delay, max–throughput, β is chosen to achieve the minimum BER, minimum delay, and maximum throughput, respectively. For opt–BER, β is chosen to minimize BER for a target delay and throughput constraint.

In Fig. 8, we show the normalized throughput vs. β for the two proposed protocols and different buffer sizes. We observe that the maximum normalized throughput for $L = 1$, is 0.5, and it increases to 1 for increasing buffer size. As β increases, the probability of selecting the $R \to D$ link P_{RD} increases which corresponds to a decrease in the throughput.

In Fig. 9, we study BER optimization for Protocol 2 with delay and throughput constraints. We assume infinite buffer size and $\bar{\gamma}_{SR} = 2\bar{\gamma}_{RD} = \bar{\gamma}$, $\rho_{SR} = 0.6$, $\rho_{RD} = 0.9$. For optimization, we assume $T_{\max} = 6$ time slots and $\tau_{\min} = 0.8\tau_0$, cf. Section VI-D. For comparison, we have shown the BER for three other cases where β is chosen to: a) minimize BER without any delay or throughput constraints (min–BER), b) minimize delay (min–delay), i.e., when $T = 1 + 2\sqrt{2}$ time slots, and c) maximize throughput, i.e., when $P_{RD} = 1/2$ and $\tau = \tau_0$. The chosen channel parameters correspond to Case *b* of Protocol 2, cf. Section (II-C). In Fig. 9, at $\bar{\gamma} = 20$ dB, $\beta = 1.614$ ($\beta = 0.80$) is numerically obtained for $P_{RD} = 1/\sqrt{2}$ ($P_{RD} = 1/2$) which corresponds to minimum delay $T_{\min} = 1 + 2\sqrt{2}$ (maximum throughput $\tau_0 = 1/2$). On the other hand, for min–BER, we obtain $\beta = 0.4$ which minimizes $P(e)$ in (18) for Case *b* for $\bar{\gamma} = 20$ dB. In Fig. 9, the error rate for min–BER is calculated analytically and shown for comparison purpose only, as we cannot operate at $\beta < 0.80$[18] to avoid buffer instability. Hence, min–BER serves as a lower bound for other protocols. At $\bar{\gamma} = 20$ dB, the value of β which gives the optimal BER (opt–BER) in Fig. 9 is 1.1, for which $T = 5$ and $\tau = 0.8\tau_0$ are obtained. Note that min–delay and max–throughput BERs correspond to $\tau = 0.5\tau_0$ and $T = \infty$, respectively. We observe that opt–BER is very close to min–BER and lower than the min–delay and max–throughput BERs.

[18] $\beta < 0.80$ would cause $P_{RD} < 1/2$, i.e., the $S \to R$ link would be chosen more often than the $R \to D$ link.

VIII. Conclusions

In this paper, we studied adaptive link selection for both perfect and outdated CSI for a three node network where the relay was equipped with a buffer. In particular, we proposed two link selection protocols based on the availability of the reliability information of the CSI estimates. We provided a unified error rate analysis for outdated and perfect CSI and showed that for perfect CSI, a diversity gain of two can be achieved, even if only a small delay can be tolerated. When the links are asymmetric, Protocol 2, which exploits the reliability information of the CSI estimates of the links, can result in a lower error rate compared to Protocol 1, for a certain target delay or throughput. We also provided closed–form expressions for the average delay and throughput for the proposed protocols for both finite and infinite buffer sizes. We showed that the decision threshold β can be chosen to satisfy different objectives, such as achieving minimum delay, maximum throughput, and minimum SER under minimum throughput and maximum delay constraints. Our results demonstrate that by appropriately choosing the value of β, it is possible to maintain buffer stability and operate close to the optimal SER at low delay with only a slight loss in throughput.

Interesting topics for future work include the analysis of the proposed modified protocol, which allows for threshold-based transmission during silent time slots, and the extension of the proposed protocols to multi-relay networks where relays forward only correctly regenerated bits.

$$P_R(e) = C\frac{\bar{\gamma}_{SR}\left(1-\sqrt{\frac{\bar{\gamma}_{SR}\eta}{2+\bar{\gamma}_{SR}\eta}}\right) - \beta\bar{\gamma}_{RD}\sqrt{\frac{\bar{\gamma}_{SR}\eta}{2+\bar{\gamma}_{SR}\eta}} + \beta\bar{\gamma}_{RD}\left(1+\frac{2}{\bar{\gamma}_{SR}\eta}+\frac{2\rho_{SR}^2}{\bar{\gamma}_{SR}\eta(1-\rho_{SR}^2)+\beta\bar{\gamma}_{RD}\eta}\right)^{-\frac{1}{2}}}{2\bar{\gamma}_{SR}}. \quad (75)$$

Appendix A
Proof of Proposition 1

We calculate the error rate conditioned on the outdated CSI as

$$P_B(e|\hat{\gamma}_{AB}) = C\int_{x=0}^{\infty}\int_{w=\sqrt{x\eta}}^{\infty} f_{\gamma_{AB}|\hat{\gamma}_{AB}}(x|y)\frac{1}{\sqrt{2\pi}}e^{-\frac{w^2}{2}}dwdx, \quad (65)$$

where $f_{\gamma_{AB}|\hat{\gamma}_{AB}}(x|y)$ is given by [18]

$$f_{\gamma_{AB}|\hat{\gamma}_{AB}}(x|y) = \frac{e^{-\frac{x+\rho_{AB}^2 y}{\bar{\gamma}_{AB}\left(1-\rho_{AB}^2\right)}}}{\bar{\gamma}_{AB}\left(1-\rho_{AB}^2\right)} I_0\left(\frac{2\sqrt{xy}\rho_{AB}}{\bar{\gamma}_{AB}\left(1-\rho_{AB}^2\right)}\right). \quad (66)$$

From (65), we obtain

$$\int_{w=\sqrt{x\eta}}^{\infty}\frac{1}{\sqrt{2\pi}}e^{-\frac{w^2}{2}}dw = \frac{1}{2}\mathrm{erfc}\left(\sqrt{\frac{x\eta}{2}}\right). \quad (67)$$

Now, combining (65)–(67), evaluating the following integral

$$C\int_{x=0}^{\infty}\frac{e^{-\frac{x+\rho_{AB}^2 y}{\bar{\gamma}_{AB}\left(1-\rho_{AB}^2\right)}}}{\bar{\gamma}_{AB}\left(1-\rho_{AB}^2\right)} I_0\left(\frac{2\sqrt{xy}\rho_{AB}}{\bar{\gamma}_{AB}\left(1-\rho_{AB}^2\right)}\right)\frac{1}{2}\mathrm{erfc}\left(\sqrt{\frac{x\eta}{2}}\right)dx \quad (68)$$

in closed–form is difficult, if not impossible. Hence, we approximate the Bessel function in (66) as

$$I_0\left(\frac{2\sqrt{xy}\rho_{AB}}{\bar{\gamma}_{AB}\left(1-\rho_{AB}^2\right)}\right) \approx 1+\left(\frac{\rho_{AB}\sqrt{xy}}{(1-\rho_{AB}^2)\bar{\gamma}_{AB}}\right)^2, \quad (69)$$

which simplifies the calculation, and leads to the simple high SNR approximation for $P_B(e|\hat{\gamma}_{AB})$ as shown in (6).

Appendix B
Proof of Proposition 2

For a RV $V \in \mathcal{N}(0,1)$, $P_B(e)$, $B \in \{R,D\}$, can be expressed as [24]

$$\begin{aligned} P_B(e) &= \mathcal{E}_{\gamma_{AB}}\Big\{\frac{C}{2}\mathrm{Pr}\Big\{\gamma_{AB} < \frac{V^2}{\eta}\Big\}\Big\} \\ &= C\int_0^{\infty} F_{\gamma_{AB}}(\frac{v^2}{\eta})f_V(v)dv, \end{aligned} \quad (70)$$

where $F_U(u)$ denotes the cumulative distribution function of U and $f_V(v) = \frac{1}{\sqrt{2\pi}}e^{-\frac{v^2}{2}}$.

Conditioned on the event $\hat{\gamma}_{SR} > \beta\hat{\gamma}_{RD}$, the average error rate of the $S \to R$ link is given by

$$\begin{aligned} P_R(e) &= \mathcal{E}\{CQ(\sqrt{\eta\gamma_{AB}})|\hat{\gamma}_{SR} > \beta\hat{\gamma}_{RD}\} \\ &= \frac{\mathcal{E}\{CQ(\sqrt{\eta\gamma_{AB}}) \cap \hat{\gamma}_{SR} > \beta\hat{\gamma}_{RD}\}}{\mathrm{Pr}(\hat{\gamma}_{SR} > \beta\hat{\gamma}_{RD})}. \end{aligned} \quad (71)$$

As mentioned in Section II-A, perfect CSI is assumed available for decoding at the receiver; only the link selection procedure has to rely on imperfect CSI. Now, for the numerator in (71), we obtain J_1

$$\begin{aligned} &\triangleq \mathcal{E}\{CQ(\sqrt{\eta\gamma_{AB}}) \cap \hat{\gamma}_{SR} > \beta\hat{\gamma}_{RD}\} \\ &= C\int_{v=0}^{\infty}\int_{x=0}^{\frac{v^2}{\eta}}\int_{y=0}^{\infty}\int_{z=0}^{\frac{y}{\beta}} f_{\gamma_{SR},\hat{\gamma}_{SR}}(x,y)f_{\hat{\gamma}_{RD}}(z) \\ &\times\ f_V(v)dz\ dy\ dx\ dv, \end{aligned} \quad (72)$$

where $f_{\hat{\gamma}_{RD}}(z) = (1/\bar{\gamma}_{RD})e^{-z/\bar{\gamma}_{RD}}$, and $f_{\gamma_{SR},\hat{\gamma}_{SR}}(x,y)$ is given in (2). After evaluating the integrals in (72), we obtain

$$\begin{aligned} J_1 &= C\frac{\bar{\gamma}_{SR}\left(1-\sqrt{\frac{\bar{\gamma}_{SR}\eta}{2+\bar{\gamma}_{SR}\eta}}\right) - \beta\bar{\gamma}_{RD}\sqrt{\frac{\bar{\gamma}_{SR}\eta}{2+\bar{\gamma}_{SR}\eta}}}{2(\bar{\gamma}_{SR}+\beta\bar{\gamma}_{RD})} \\ &+ \frac{C\beta\bar{\gamma}_{RD}}{2(\bar{\gamma}_{SR}+\beta\bar{\gamma}_{RD})\sqrt{1+\frac{2}{\bar{\gamma}_{SR}\eta}+\frac{2\rho_{SR}^2}{\bar{\gamma}_{SR}\eta(1-\rho_{SR}^2)+\beta\bar{\gamma}_{RD}\eta}}}. \end{aligned} \quad (73)$$

Furthermore, for the denominator in (71), we obtain

$$\begin{aligned} P_{SR} &\triangleq \mathrm{Pr}(\hat{\gamma}_{SR} > \beta\hat{\gamma}_{RD}) = \int_{y=0}^{\infty}\int_{x=\beta y}^{\infty} f_{\hat{\gamma}_{SR}}(x)f_{\hat{\gamma}_{RD}}(y)dx\ dy \\ &= \frac{\bar{\gamma}_{SR}}{\bar{\gamma}_{SR}+\beta\bar{\gamma}_{RD}}. \end{aligned} \quad (74)$$

Now, combining (71), (73) and (74), we obtain $P_R(e)$ in (75). Similarly, we can derive the expression for $P_D(e)$. Combining $P_R(e)$ and $P_D(e)$, we obtain $P(e)$ in (13). The error rate for perfect CSI can be obtained by setting $\rho_{SR} = \rho_{RD} = 1$ in (13). This concludes the proof.

Appendix C
Proof of Proposition 3

Here, we provide the proof of Proposition 3. In particular, we provide the derivation for Case *a*. The expressions for Case *b* can be obtained following a similar approach and are omitted here. We obtain the unconditional error rate $P_R(e)$ by averaging $P_R(e|\hat{\gamma}_{SR})$ (cf. (6)) as $P_R(e)$

$$= \mathcal{E}_{\hat{\gamma}_{SR},\hat{\gamma}_{RD}}\{P(e|\hat{\gamma}_{SR} \geq l_1)\} = \frac{\mathcal{E}\{P_R(e,\hat{\gamma}_{SR} \geq l_1)\}}{\mathrm{Pr}(\hat{\gamma}_{SR} \geq l_1)} = \frac{J_2}{P_{SR}}, \quad (76)$$

where J_2 is given by

$$\begin{aligned} J_2 &= \mathcal{E}\{P_R(e,\hat{\gamma}_{SR} \geq l_1)\} \\ &= C\int_{z=0}^{\infty}\int_{y=l_1}^{\infty}\frac{1}{\mu_{SR}}e^{-\frac{y\rho_{SR}^2}{\bar{\gamma}_{SR}(1-\rho_{SR}^2)}} f_{\hat{\gamma}_{SR}}(y)f_{\hat{\gamma}_{RD}}(z)dydz, \end{aligned} \quad (77)$$

where l_1 was defined in (9). Evaluating the integrals in (77), we obtain J_2 as

$$J_2 = C\frac{\rho_{SR}^2\left(\frac{\mu_{RD}}{\mu_{SR}}\right)^{-1/\rho_{SR}^2}(1-\rho_{SR}^2)(1-\rho_{RD}^2)}{\mu_{SR}(\beta\rho_{RD}^2+\rho_{SR}^2(1-\rho_{RD}^2))}. \quad (78)$$

Similar to (74) for Protocol 1, we obtain P_{SR}, the probability of selecting the $S \to R$ link, for Protocol 2 and Case *a* as

$$P_{SR} \triangleq \Pr(\hat{\gamma}_{SR} \geq l_1) = \frac{\rho_{SR}^2 \left(\frac{\mu_{RD}}{\mu_{SR}}\right)^{-1/\rho_{SR}^2} (1-\rho_{RD}^2)}{\beta\rho_{RD}^2 + \rho_{SR}^2(1-(1+\beta)\rho_{RD}^2)}. \tag{79}$$

Similarly, the unconditional error rate of the $R \rightarrow D$ link is obtained as

$$P_D(e) = \frac{\mathcal{E}\{P_D(e, \hat{\gamma}_{SR} < l_1)\}}{\Pr(\hat{\gamma}_{SR} < l_1)} = \frac{J_3}{P_{RD}}, \tag{80}$$

where J_3

$$\begin{aligned} &\triangleq C\int_{z=0}^{\infty}\int_{y=0}^{l_1} \frac{1}{\mu_{RD}} e^{-\frac{\beta z \rho_{RD}^2}{\bar{\gamma}_{RD}(1-\rho_{RD}^2)}} f_{\hat{\gamma}_{SR}}(y) f_{\hat{\gamma}_{RD}}(z) dydz \\ &= C\left(\frac{1-\rho_{RD}^2}{\mu_{RD}} - \frac{\left(\frac{\mu_{RD}}{\mu_{SR}}\right)^{-1/\rho_{SR}^2} \rho_{SR}^2(1-\rho_{RD}^2)}{\mu_{SR}(\rho_{SR}^2 + \beta(1-\rho_{SR}^2)\rho_{RD}^2)}\right). \end{aligned} \tag{81}$$

Next, the probability of selecting the $R \rightarrow D$ link $P_{RD} = \Pr(\hat{\gamma}_{SR} < l_1)$ for Protocol 2 and Case a) is obtained as

$$P_{RD} = \Pr(\hat{\gamma}_{SR} < l_1) = 1 - \frac{\left(\frac{\mu_{RD}}{\mu_{SR}}\right)^{1-1/\rho_{SR}^2} \rho_{SR}^2(1-\rho_{RD}^2)}{\beta\rho_{RD}^2 + \rho_{SR}^2(1-(1+\beta)\rho_{RD}^2)}. \tag{82}$$

Now, combining (76)–(82), the end–to–end unconditional SER can be obtained as shown in (18).

References

[1] T. Islam, D. S. Michalopoulos, R. Schober, and V. Bhargava, “Delay Constrained Buffer–Aided Relaying with Outdated CSI,” in *Proc. IEEE WCNC*, Istanbul, Turkey, Apr. 2014.

[2] J. Laneman, D. Tse, and G. Wornell, “Cooperative Diversity in Wireless Networks: Efficient Protocols and Outage Behavior,” *IEEE Trans. Inform. Theory*, vol. 50, pp. 3062–3080, Sep. 2004.

[3] A. Sendonaris, E. Erkip, and B. Aazhang, “User Cooperation Diversity – Parts I and II,” *IEEE Trans. Commun.*, vol. 51, pp. 1927–1948, Nov. 2003.

[4] N. Zlatanov, A. Ikhlef, T. Islam, and R. Schober, “Buffer–Aided Cooperative Communications: Opportunities and Challenges,” *IEEE Commun. Magazine*, vol. 52, pp. 146–153, Apr. 2014.

[5] B. Xia, Y. Fan, J. Thompson, and H. V. Poor, “Buffering in a Three Node Relay Network,” *IEEE Trans. Wireless Commun.*, vol. 7, pp. 4492–4496, Nov. 2008.

[6] L. Ding, M. Tao, F. Yang, and W. Zhang, “Joint Scheduling and Relay Selection in One– and Two–Way relay Networks with Buffering,” in *Proc. IEEE ICC*, Dresden, Germany, 2009.

[7] N. Zlatanov, R. Schober, and P. Popovski, “Buffer–Aided Relaying with Adaptive Link Selection,” *IEEE J. Select. Areas Commun.*, vol. 31, pp. 1530–1542, Aug. 2013.

[8] N. Zlatanov and R. Schober, “Buffer–Aided Relaying with Adaptive Link Selection – Fixed and Mixed Rate Transmission,” *IEEE Trans. Inform. Theory*, vol. 59, pp. 2816 – 2840, May 2013.

[9] R. Wang, V. K. Lau, and H. Huang, “Opportunistic Buffered Decode–Wait–and–Forward (OBDWF) Protocol for Mobile Wireless Relay Networks,” *IEEE Trans. Wireless Commun.*, vol. 10, pp. 1224–1231, Apr. 2011.

[10] N. Zlatanov and R. Schober, “Buffer–Aided Half–Duplex Relaying Can Outperform Ideal Full–Duplex Relaying,” *IEEE Commun. Lett.*, vol. 17, pp. 479–482, Mar. 2013.

[11] A. Ikhlef, D. S. Michalopoulos, and R. Schober, “Max–Max Relay Selection for Relays with Buffers,” *IEEE Trans. Wireless Commun.*, vol. 11, pp. 1124–1135, Mar. 2012.

[12] A. Ikhlef, J. Kim, and R. Schober, “Mimicking Full-Duplex Relaying Using Half-Duplex Relays With Buffers,” *IEEE Trans. Veh. Technol.*, vol. 61, pp. 3025–3037, Sep. 2012.

[13] I. Krikidis, T. Charalambous, and J. S. Thompson, “Buffer–Aided Relay Selection for Cooperative Diversity Systems without Delay Constraints,” *IEEE Trans. Wireless Commun.*, vol. 11, pp. 1957–1967, May 2012.

[14] C. Dong, L.-L. Yiang, and L. Hanzo, “Performance Analysis of Multihop–Diversity–Aided Multihop Links,” *IEEE Trans. Veh. Technol.*, vol. 61, pp. 2504–2516, Jul. 2012.

[15] G.-X. Li, C. Dong, D. Liu, G. Li, and Y. Zhang, “Outage Analysis of Dual–Hop Transmission with Buffer Aided Amplify–and–Forward Relay,” in *Proc. IEEE VTC–Fall*, Vancouver, Sep. 2014.

[16] J. L. Vicario, A. Bel, J. A. Lopez-Salcedo, and G. Seco, “Opportunistic Relay Selection with Outdated CSI: Outage Probability and Diversity Analysis,” *IEEE Trans. Wireless Commun.*, vol. 8, pp. 2872–2876, Jun. 2009.

[17] M. Torabi, D. Haccoun, and J. F. Frigon, “Impact of Outdated Relay Selection on the Capacity of AF Opportunistic Relaying Systems with Adaptive Transmission over Non–Identically Distributed Links,” *IEEE Trans. Wireless Commun.*, vol. 10, pp. 3626–3631, Nov. 2011.

[18] D. S. Michalopoulos, H. A. Suraweera, G. K. Karagiannidis, and R. Schober, “Amplify–and–Forward Relay Selection with Outdated Channel Estimates,” *IEEE Trans. Commun.*, vol. 60, pp. 1278– 1290, Jun. 2012.

[19] B. Zhong, Z. Zhang, X. Zhang, Y. Li, and K. Long, “Impact of Partial Relay Selection on the Capacity of Communications Systems with Outdated CSI and Adaptive Transmission Techniques,” *EURASIP Journal on Wireless Communications and Networking*, 2013, 2013:24, 13 pages.

[20] T. Islam, A. Ikhlef, R. Schober, and V. K. Bhargava, “Diversity and Delay Analysis of Buffer–Aided BICM–OFDM Relaying,” *IEEE Trans. Wireless Commun.*, vol. 12, pp. 5506–5519, Nov. 2013.

[21] E. W. C. Jakes, Jr., *Microwave Mobile Communications*. New Jersey: Prentice–Hall, 1974.

[22] T. Wang, A. Cano, G. B. Giannakis, and J. N. Laneman, “High-Performance Cooperative Demodulation with Decode-and-Forward Relays,” *IEEE Trans. Commun.*, vol. 55, pp. 1427– 1438, Jul. 2007.

[23] T. Wang, G. Giannakis, and R. Wang, “Smart Regenerative Relays for Link-Adaptive Cooperation,” *IEEE Trans. Commun.*, vol. 56, pp. 1950–1960, Nov. 2008.

[24] Y. Zhao, R. Adve, and T. Lim, “Symbol Error Rate of Selection Amplify–and–Forward Relay Systems,” *IEEE Commun. Lett.*, vol. 10, pp. 757–759, Nov. 2006.

[25] P. Kalansuriya and C. Tellambura, “Performance Analysis of Decode–and–Forward Relay Network under Adaptive M–QAM,” in *Proc. IEEE ICC*, Dresden, Germany, Jun. 2009.

[26] A. Papoulis, *Probability, Random Variables and Stochastic Processes*. New York: McGraw–Hill, 1984.

Toufiqul Islam (S’10, M’15) received his B.Sc. and M.Sc. degrees in Electrical and Electronic Engineering from Bangladesh University of Engineering and Technology, Dhaka, Bangladesh, in 2006 and 2008, respectively. He obtained the Ph.D. degree in Electrical and Computer Engineering at The University of British Columbia (UBC), Vancouver, Canada in 2014. He is now a Research Engineer at the Huawei Canada Research Center, Ottawa, Canada.

His research interests include flexible air–interface for 5G, wireless caching, buffer–aided relaying, and applications of machine learning techniques in communications. He has won the Donald N. Byers Prize, the highest graduate student honor at the UBC. He was also the recipient of the prestigious Vanier Canada Graduate Scholarship, the Killam Doctoral Fellowship, and the UBC Four Year Fellowship in 2011, 2010, and 2009, respectively. He was one of the six finalists for the 2015 Governor General Gold Medal at the UBC. Sponsored by a competitive German Academic Exchange Service (DAAD) research grant and the NSERC Michael Smith Foreign Study Supplements program, he visited the Institute of Digital Communications at the Friedrich Alexander University (FAU), Erlangen, Germany during the Summer of 2013. His paper was awarded 2nd prize in the IEEE Region 10 undergraduate student paper contest in 2006. He also won the IEEE Globecom 2012 travel grant award.

Diomidis S. Michalopoulos (S'05, M'10, SM'15) was born in Thessaloniki, Greece, in 1983. He received the Diploma in engineering (5 year studies) and the Ph.D. degree from the Electrical and Computer Engineering Department, Aristotle University of Thessaloniki, in 2005 and 2009, respectively. In 2009, he joined the University of British Columbia, Canada, as a Killam postdoctoral fellow, and in 2011, he was awarded a Banting postdoctoral fellowship. From Feb. 2014 to Apr. 2015 he was with the University of Erlangen–Nuremberg, Germany, as researcher and teaching instructor. Since May 2015 he is with Nokia Networks, Germany, as Radio Systems Research Engineer.

His research interests span the broad area of digital wireless communications, with emphasis on physical layer as well as radio access aspects. Dr. Michalopoulos received the Marconi Young Scholar award from the Marconi Society in 2010, the Killam postdoctoral fellow research prize for excellence in research in the University of British Columbia in 2011, and the Best Paper Award of the Wireless Communications Symposium (WCS) in the IEEE International Conference on Communications (ICC'07). He has served as member of Technical Program Committees for major IEEE conferences such as Globecom, WCNC, and VTC. He is also an Associate Editor of the IEEE Communications Letters.

Robert Schober (M'01, SM'08, F'10) was born in Neuendettelsau, Germany, in 1971. He received the Diplom (Univ.) and the Ph.D. degrees in electrical engineering from the University of Erlangen–Nuermberg in 1997 and 2000, respectively. From May 2001 to April 2002 he was a Postdoctoral Fellow at the University of Toronto, Canada, sponsored by the German Academic Exchange Service (DAAD). Since May 2002 he has been with the University of British Columbia (UBC), Vancouver, Canada, where he is now a Full Professor and Canada Research Chair (Tier II) in Wireless Communications. Since January 2012, he is an Alexander von Humboldt Professor and the Chair for Digital Communication at the Friedrich Alexander University (FAU), Erlangen, Germany. His research interests fall into the broad areas of Communication Theory, Wireless Communications, and Statistical Signal Processing.

Dr. Schober received several awards for his work including the 2002 Heinz Maier–Leibnitz Award of the German Science Foundation (DFG), the 2004 Innovations Award of the Vodafone Foundation for Research in Mobile Communications, the 2006 UBC Killam Research Prize, the 2007 Wilhelm Friedrich Bessel Research Award of the Alexander von Humboldt Foundation, the 2008 Charles McDowell Award for Excellence in Research from UBC, a 2011 Alexander von Humboldt Professorship, and a 2012 NSERC E. W. R. Steacie Fellowship. In addition, he received best paper awards from the German Information Technology Society (ITG), the European Association for Signal, Speech and Image Processing (EURASIP), IEEE WCNC 2012, IEEE Globecom 2011, IEEE ICUWB 2006, the International Zurich Seminar on Broadband Communications, and European Wireless 2000. Dr. Schober is a Fellow of the IEEE, the Canadian Academy of Engineering, and the Engineering Institute of Canada. He is currently the Editor–in–Chief of the IEEE TRANSACTIONS ON COMMUNICATIONS.

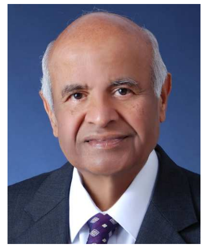

Vijay K. Bhargava (M'74, SM'82, F'92) Vijay Bhargava was born in Beawar, India in 1948. He came to Canada in 1966 and obtained BASc, MASc and PhD degrees from Queen's University at Kingston in 1970, 1972 and 1974 respectively. He is a Professor in the Department of Electrical and Computer Engineering at the University of British Columbia in Vancouver, where he served as Department Head during 2003–2008. Previously he was with the University of Victoria (1984–2003), Concordia University (1976–1984), the University of Waterloo (1976) and the Indian Institute of Science (1974-1975). He has held visiting appointments at Ecole Polytechnique de Montreal, NTT Research Lab, Tokyo Institute of Technology, the University of Indonesia, the Hong Kong University of Science and Technology, and Tohoku University. He is an Honourary Professor at UESTC, Chengdu and a Gandhi Distinguished Professor at IIT Bombay. Currently he is on sabbatical leave at the Friedrich-Alexander University Erlangen–Nuremberg. He is in the Institute for Scientific Information (ISI) Highly Cited list.

Vijay served as the Founder and President of "Binary Communications Inc." (1983–2000). He is a co-author (with D. Haccoun, R. Matyas and P. Nuspl) of "Digital Communications by Satellite" (New York: Wiley: 1981) which was translated in Chinese and Japanese. He is a co-editor (with S. Wicker) of "Reed Solomon Codes and their Applications" (IEEE Press: 1994), a co-editor (with H.V. Poor, V. Tarokh and S. Yoon) of "Communications, Information and Network Security" (Kluwer: 2003) a co-editor (with E. Hossain) of "Cognitive Wireless Communication Networks" (Springer: 2007), a co-editor (with E. Hossain and D.I Kim) of "Cooperative Wireless Communications Networks", (Cambridge University Press: 2011) and a co–editor (with E. Hossain and G. Fettweis) of "Green Radio Communications Networks" (Cambridge University Press 2012).

Vijay is a Fellow of the IEEE, The Royal Society of Canada, The Canadian Academy of Engineering and the Engineering Institute of Canada. He is a Foreign Fellow of the National Academy of Engineering (India) and has served as a Distinguished Visiting Fellow of the Royal Academy of Engineering (U.K.). He is a recipient of the 2015 Killam prize in Engineering awarded by the Canada Council and a Humboldt Research Award from the Alexander von Humboldt Stiftung.

Vijay has served as the editor–in–chief (2007–2009) of the IEEE Transactions on Wireless Communications. He is a past President of the IEEE Information Theory Society and a Past President of the IEEE Communications Society.